

Active learning for level set estimation under cost-dependent input uncertainty

Yu Inatsu ^{*} Masayuki Karasuyama ^{†‡§} Keiichi Inoue [¶] Ichiro Takeuchi ^{*†§||}

September 16, 2019

ABSTRACT

As part of a quality control process in manufacturing it is often necessary to test whether all parts of a product satisfy a required property, with as few inspections as possible. When multiple inspection apparatuses with different costs and precision exist, it is desirable that testing can be carried out cost-effectively by properly controlling the trade-off between the costs and the precision. In this paper, we formulate this as a level set estimation (LSE) problem under cost-dependent input uncertainty – LSE being a type of active learning for estimating the level set, i.e., the subset of the input space in which an unknown function value is greater or smaller than a pre-determined threshold. Then, we propose a new algorithm for LSE under cost-dependent input uncertainty with theoretical convergence guarantee. We demonstrate the effectiveness of the proposed algorithm by applying it to synthetic and real datasets.

1. Introduction

In this paper, we consider a type of active learning (AL) problem called *level set estimation (LSE)* [4]. The goal of LSE is to efficiently identify the *level set* $\{\mathbf{x} \in D \mid f(\mathbf{x}) > h\}$ of an unknown high-cost real-valued function $f : D \rightarrow \mathbb{R}$, i.e., the input region in which the function output $f(\mathbf{x})$ is greater than a threshold h . LSE plays an important role in quality control processes in manufacturing, because engineers want to ensure that all parts of a product satisfy the required properties with as few inspections as possible. For example, the task of extracting a region satisfying a required physical property from a solid material can be formulated as an LSE problem. In order to investigate a physical property, each position of a solid material is subjected to X-ray irradiation. Since X-ray irradiation is costly, it is desirable to find the level set (a region in the solid material in which the required physical properties are satisfied) with as few rounds of X-ray irradiation as possible. We also encounter an LSE problem in bio-engineering, e.g., in the task of constructing new functional proteins such as drugs or foods, by artificially modifying amino acid sequences of proteins. Here, bio-engineers need to identify the level set (the region in the protein feature space in which the protein satisfies the required functional properties) by repeatedly modifying amino acid sequences of proteins.

When LSE is used for such manufacturing quality control process, trade-offs between the input uncertainty and the cost are often taken into account. For instance, in the first example, it is necessary to use a high-cost X-ray irradiation apparatus in order to accurately irradiate the X-ray to the correct position of the solid material, while alternative low-cost X-ray irradiation apparatuses are also available, although they generally cannot irradiate the target position as precisely as higher cost ones. In the second example, precise modification of amino acids at precise positions is more expensive than a random mutation approach in which amino acids in a certain range of positions are replaced at random. In such a situation, it is desirable to be able to guarantee the quality of the entire product with as little total cost as possible by effectively combining low cost function evaluation that have high input uncertainty, with high cost function evaluation that have low input uncertainty.

The basic strategy of conventional AL methods is to select the inputs in which the uncertainty reduction of the corresponding outputs is beneficial to the target task (see, e.g., [16]). Unfortunately, under

^{*}RIKEN Center for Advanced Intelligence Project

[†]Nagoya Institute of Technology

[‡]JST, PRESTO

[§]Center for Materials Research by Information Integration, National Institute for Materials Science

[¶]University of Tokyo

^{||}E-mail:takeuchi.ichiro@nitech.ac.jp

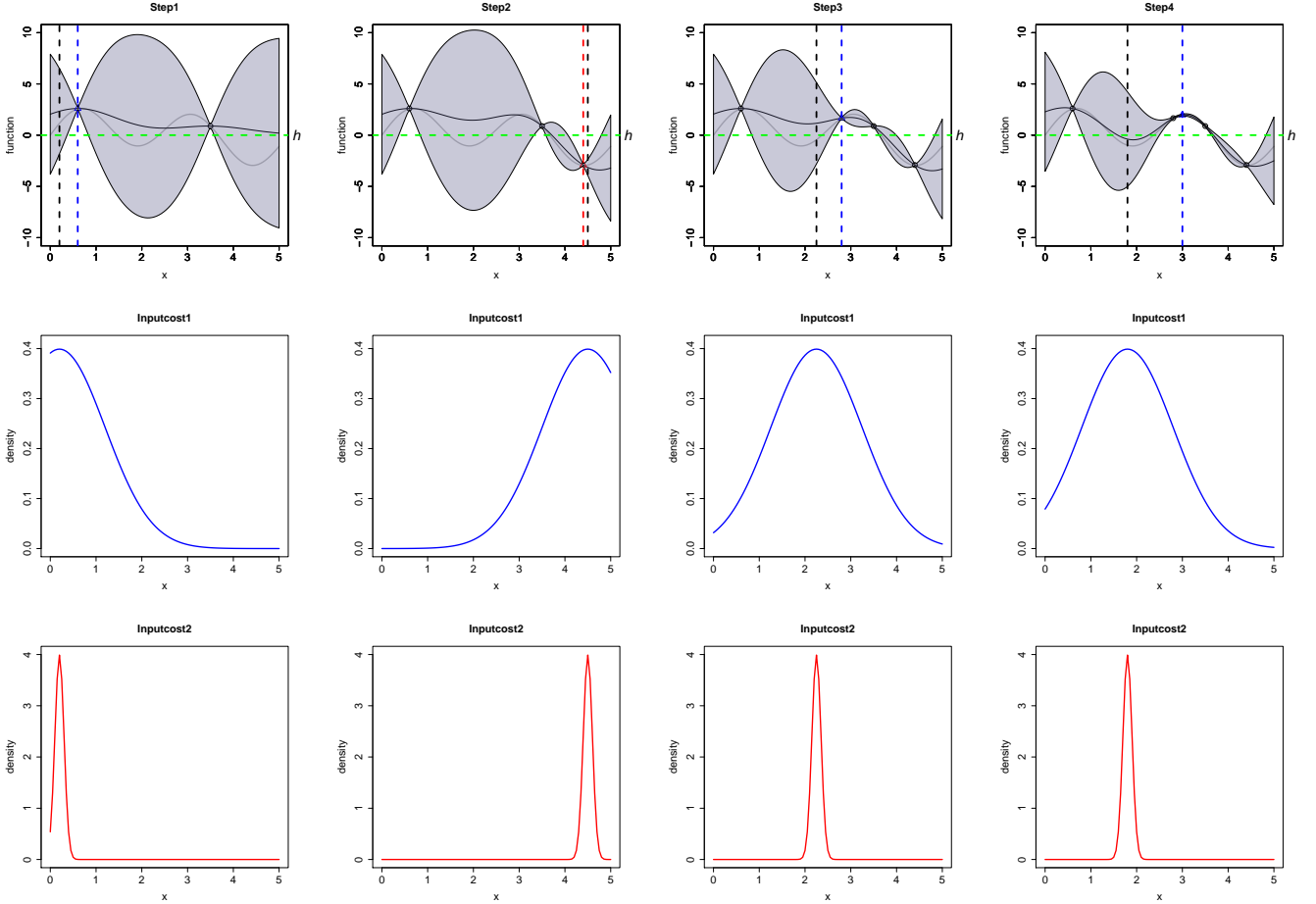


Figure 1: An illustration of LSE problem with cost-dependent input uncertainty: an example of Gaussian Process (GP) model-based LSE with two different function evaluation options where option 1 has a low cost but high input uncertainty (middle row plots), while option 2 has a high cost but low input uncertainty (bottom row plots). In the top row plots, the black dashed lines indicate the desired input points, whereas the blue and red dashed lines indicate the actual input points due to input uncertainty. In this example, option 1 (low cost with large input uncertainty) were selected in steps 1, 3, and 4, whereas option 2 (high cost with small input uncertainty) were selected in step 2. The choices of option 1 in steps 1 and 3 (as well as the choice of option 2 in step 2) were effective in the sense that the uncertainty of the GP model was effectively reduced. On the other hand, the choice of option 1 in step 4 was not effective because the function was evaluated at highly different input point and the uncertainty of the GP model could not be effectively reduced. This example illustrates that, in LSE problems with cost-dependent input uncertainty, the proper choice of function evaluation options is important.

input uncertainty, this basic AL strategy cannot be used as it is because the input point cannot be freely specified. In fact, the convergence of existing LSE methods such as [8, 28] cannot be guaranteed under input uncertainty. In this paper, we propose a cost-sensitive AL method for LSE with input uncertainty by properly taking into account the *integrated uncertainty* according to the input uncertainty distribution, i.e., by precisely evaluating how the uncertainty of an unknown function decreases using an integral calculation with respect to the input uncertainty. We first consider the case in which the input uncertainty distribution is known, and then extend the result to the case in which the input uncertainty distribution is unknown. We investigate the theoretical properties of the proposed LSE method and show that it can identify the true level set with high probability under certain conditions. Furthermore, through numerical experiments using artificial and real datasets, we demonstrate the effectiveness of the proposed method.

1.1. Related works

Bayesian optimization (BO) based on Bayesian inference has been used for various target tasks including LSE (see [17] for comprehensive survey of BO). Several LSE methods based on Gaussian Process (GP) model have been studied. For example, [4] proposed the STRADDLE strategy based on credible intervals. In addition, [8] proposed an LSE method using a confidence region which is the intersection of credible intervals and derived theoretical bounds. Furthermore, recently, [28] proposed an LSE method called MILE based on the expected classification improvement, and [19] proposed a new LSE with tighter theoretical bounds and lower computational costs. Similarly, [3] has proposed a method for combining the maximization problem and LSE, and [22, 23, 25, 26] have used LSE for efficient safety area identification. There are several existing studies dealing with input uncertainty in GP model. Recently, [1] has considered BO for minimizing an integral function which is computed by integrating an unknown function with respect to input distributions, and [11] has proposed an upper confidence bound algorithm under uncertainty inputs. Moreover, in the framework of time series analysis, [7] has proposed an acquisition function based on the integral with respect to input distributions. Furthermore, in the context of Bayesian quadrature (see, e.g., [10]), [27, 6] proposed a method for efficiently computing the target integral value with respect to input distributions. These existing studies on input uncertainty have some similarities with our study in that they are all based on integral calculations of input uncertainty distributions, but these existing techniques cannot be directly used for LSE under input uncertainty. Although there are many existing studies on cost-sensitive BOs (e.g., [24, 20, 12, 15]), they all considered cost-dependent precision of GP models and none of them deal with cost-dependent input uncertainty.

1.2. Contributions

Our main contributions in this paper are as follows:

- We propose a new active learning algorithm for LSE problems under cost-dependent input uncertainty by extending the recent LSE method in [28].
- We show the convergence of the proposed algorithm, i.e., the desired level set can be identified with probability one under certain regularity conditions. Moreover, we also show that the number of necessary function evaluation for level set identification was finite with probability one.
- Through numerical experiments using synthetic data and real data, we confirm that our proposed method has the same or better performance than other methods.

2. Preliminaries

Let $f : D \rightarrow \mathbb{R}$ be a black-box function on $D \subset \mathbb{R}^d$ with expensive to evaluate. For each $\mathbf{x} \in D$, assume that the value of $f(\mathbf{x})$ can be observed as $f(\mathbf{x}) + \varrho$, where ϱ is an independent Gaussian noise distributed as $\mathcal{N}(0, \sigma^2)$. In this paper, we consider an LSE problem for f on a finite subset Ω of D . The upper and lower level sets for f on Ω at threshold h are defined as follows:

Definition 2.1. Let h be a threshold. Then, an upper level set H and a lower level set L are defined as

$$H = \{\mathbf{x} \in \Omega \mid f(\mathbf{x}) > h\}, \quad L = \{\mathbf{x} \in \Omega \mid f(\mathbf{x}) \leq h\}.$$

In this paper, we consider cost-dependent input uncertainties when the black-box function f is evaluated. Assume that we have k different options (equipments/apparatus) for evaluating f , and these options have different costs $c_1 < c_2 \cdots < c_k$. When an option $i \in [k]$ is used for evaluating f at an $\mathbf{x} \in \Omega$, the actual function evaluation is done not exactly at \mathbf{x} but at $\mathbf{s}(\mathbf{x}, c_i) \in D$ where $\mathbf{s}(\mathbf{x}, c_i)$ is considered as a random sample from a random variable $\mathbf{S}(\mathbf{x}, c_i)$. Since there is a trade-off between the costs and the input uncertainties, we need to select appropriate function evaluation options from the k different choices at each step. In this paper, we first assume that the probability density function of $\mathbf{S}(\mathbf{x}, c_i)$, denoted by $g(\mathbf{s} \mid \boldsymbol{\theta}_{\mathbf{x}}^{(c_i)})$ with parameters $\boldsymbol{\theta}_{\mathbf{x}}^{(c_i)}$, is known¹, but later extends to the case where the parameters is unknown and must be estimated in §4.

¹Note that we assume that $\mathbf{S}(\mathbf{x}, c_i)$ is a continuous random variable, but the discussion in this paper can be applied even if $\mathbf{S}(\mathbf{x}, c_i)$ is discrete. In that case, the integration operation in Section 3 must be replaced with a summation operation.

2.1. Gaussian process

In this paper, GP is used for modeling the black-box function f . Let $\mathcal{GP}(0, k(\mathbf{s}, \mathbf{s}'))$ be a GP prior for the function f , where $k(\mathbf{s}, \mathbf{s}') : D \times D \rightarrow \mathbb{R}$ is a positive-definite kernel. Therefore, for any pair of finite points $\mathbf{s}_1, \dots, \mathbf{s}_t \in D$ and its values $f(\mathbf{s}_1), \dots, f(\mathbf{s}_t)$, a joint distribution of $(f(\mathbf{s}_1), \dots, f(\mathbf{s}_t))^\top$ is given by $\mathcal{N}_t(\boldsymbol{\mu}_t, \mathbf{K}_t)$, where $\mathcal{N}_t(\boldsymbol{\mu}_t, \mathbf{K}_t)$ is a t -dimensional normal distribution with mean vector $\boldsymbol{\mu}_t$ and covariance matrix \mathbf{K}_t , $\boldsymbol{\mu}_t = (0, \dots, 0)^\top \equiv \mathbf{0}_t$, and the (i, j) element of \mathbf{K}_t is $k(\mathbf{s}_i, \mathbf{s}_j)$. From the properties of GP, a posterior distribution of f after adding the data set $\{(\mathbf{s}_j(\mathbf{x}_j, c_{i_j}), y_j)\}_{j=1}^t$ is also GP. Then, a posterior mean $\mu_t(\mathbf{x})$, variance $\sigma_t^2(\mathbf{x})$ and covariance $k_t(\mathbf{x}, \mathbf{x}')$ of f at \mathbf{x} are given by

$$\mu_t(\mathbf{x}) = \mathbf{k}_t(\mathbf{x})^\top \mathbf{C}_t^{-1} \mathbf{y}_t, \sigma_t^2(\mathbf{x}) = k_t(\mathbf{x}, \mathbf{x}), k_t(\mathbf{x}, \mathbf{x}') = k(\mathbf{x}, \mathbf{x}') - \mathbf{k}_t(\mathbf{x})^\top \mathbf{C}_t^{-1} \mathbf{k}_t(\mathbf{x}'),$$

where $\mathbf{k}_t(\mathbf{x}) = (k(\mathbf{s}_1(\mathbf{x}_1, c_{i_1}), \mathbf{x}), \dots, k(\mathbf{s}_t(\mathbf{x}_t, c_{i_t}), \mathbf{x}))^\top$, $\mathbf{C}_t = (\mathbf{K}_t + \sigma^2 \mathbf{I}_t)$, $\mathbf{y}_t = (y_1, \dots, y_t)^\top$, and \mathbf{I}_t is a t -dimensional identity matrix.

3. Proposed method

In this section, we propose an efficient AL method for LSE under cost-dependent input uncertainty.

3.1. Credible interval and LSE

For each $\mathbf{x} \in \Omega$, let $Q_t(\mathbf{x}) = [l_t(\mathbf{x}), u_t(\mathbf{x})]$ be a credible interval of $f(\mathbf{x})$ at the t th trial, where $l_t(\mathbf{x}) = \mu_t(\mathbf{x}) - \beta^{1/2} \sigma_t(\mathbf{x})$, $u_t(\mathbf{x}) = \mu_t(\mathbf{x}) + \beta^{1/2} \sigma_t(\mathbf{x})$, and $\beta^{1/2} \geq 0$. In addition, let ϵ be a positive accuracy parameter. Then, we define estimated sets H_t and L_t respectively of H and L as

$$H_t = \{\mathbf{x} \in \Omega \mid l_t(\mathbf{x}) > h - \epsilon\}, L_t = \{\mathbf{x} \in \Omega \mid u_t(\mathbf{x}) < h + \epsilon\}. \quad (3.1)$$

Moreover, we define an unclassified set $U_t = \Omega \setminus (H_t \cup L_t)$. Each step of LSE can be interpreted as the problem of classifying $\mathbf{x} \in U_{t-1}$ into H_t or L_t .

3.2. Acquisition function

Here, we propose an acquisition function to determine the next input point and the evaluation cost of the input point. We extend the MILE acquisition function proposed by [28]. MILE is based on the idea that the next evaluation point is the point that maximizes the expected classification improvement when a new point is added. Since inputs have cost-dependent uncertainty in our setting, we consider the *integral* with respect to the input distribution of the expected classification improvement, and define the integral divided by the cost as our acquisition function value. Moreover, by using the randomized strategy, we can show that our proposed algorithm converges with probability 1.

3.2.1. Integral with respect to input of expected classification improvement per unit cost

Let $\mathbf{s}^* \in D$ be a new point, and let $y^* = f(\mathbf{s}^*) + \varrho$ be the observed value for \mathbf{s}^* . In addition, let $H_t(\mathbf{s}^*, y^*)$ and $L_t(\mathbf{s}^*, y^*)$ be estimated sets respectively of H and L when (\mathbf{s}^*, y^*) is added, and let $HL_t(\mathbf{s}^*, y^*) = H_t(\mathbf{s}^*, y^*) \cup L_t(\mathbf{s}^*, y^*)$, $HL_t = H_t \cup L_t$. Then, when the observation cost of the input point $\mathbf{x} \in \Omega$ is c_i , the integral of the expected classification improvement per unit cost is given by

$$a_t(\mathbf{x}, c_i) = c_i^{-1} \left\{ \int \mathbb{E}_{y^*} [|HL_t(\mathbf{s}^*, y^*)|] g(\mathbf{s}^* | \theta_{\mathbf{x}}^{(c_i)}) d\mathbf{s}^* - |HL_t| \right\}. \quad (3.2)$$

Furthermore, the expectation in (3.2) can be written as follows:

Lemma 3.1. The expectation in (3.2) can be written as

$$\mathbb{E}_{y^*} [|HL_t(\mathbf{s}^*, y^*)|] = \sum_{\mathbf{a} \in \Omega} \Phi \left(\frac{\sqrt{\sigma_t^2(\mathbf{s}^*) + \sigma^2}}{|k_t(\mathbf{a}, \mathbf{s}^*)|} \times c_t^+(\mathbf{a} | \mathbf{s}^*) \right) + \sum_{\mathbf{a} \in \Omega} \Phi \left(\frac{\sqrt{\sigma_t^2(\mathbf{s}^*) + \sigma^2}}{|k_t(\mathbf{a}, \mathbf{s}^*)|} \times c_t^-(\mathbf{a} | \mathbf{s}^*) \right).$$

Here, $c_t^+(\mathbf{a} | \mathbf{s}^*) = \mu_t(\mathbf{a}) - \beta^{1/2} \sigma_t(\mathbf{a} | \mathbf{s}^*) - h + \epsilon$, $c_t^-(\mathbf{a} | \mathbf{s}^*) = -\mu_t(\mathbf{a}) - \beta^{1/2} \sigma_t(\mathbf{a} | \mathbf{s}^*) + h + \epsilon$, and $\sigma_t^2(\mathbf{a} | \mathbf{s}^*)$ is the posterior variance of f at the point \mathbf{a} after adding \mathbf{s}^* to $\{(\mathbf{s}_j(\mathbf{x}_j, c_{i_j}), y_j)\}_{j=1}^t$. Moreover, when $k_t(\mathbf{a}, \mathbf{s}^*) = 0$,

Algorithm 1 LSE under cost dependent input uncertainty

Input: Initial training data, GP prior $\mathcal{GP}(0, k(\mathbf{x}, \mathbf{x}'))$, probabilities $\{p_t\}_{t \in \mathbb{N}}$, $\{\kappa_j\}_{j=1}^k$

Output: Estimated sets \widehat{H} and \widehat{L}

```
1:  $\widehat{H}_0 \leftarrow \emptyset, \widehat{L}_0 \leftarrow \emptyset, U_0 \leftarrow \Omega$ 
2:  $t \leftarrow 1$ 
3: while  $U_{t-1} \neq \emptyset$  do
4:    $\widehat{H}_t \leftarrow \widehat{H}_{t-1}, \widehat{L}_t \leftarrow \widehat{L}_{t-1}, U_t \leftarrow U_{t-1}$ 
5:   for all  $\mathbf{x} \in \Omega$  do
6:     Compute credible interval  $Q_t(\mathbf{x})$  from GP
7:   end for
8:   Compute  $H_t, L_t$  and  $U_t$  from (3.1) and generate  $r_t$  from  $\mathcal{B}(p_t)$ 
9:   if  $r_t = 0$  then
10:     $(\mathbf{x}_t, c_{i_t}) = \operatorname{argmax}_{(\mathbf{x}, c_i)} a_t(\mathbf{x}, c_i)$ 
11:   else if  $r_t = 1$  then
12:    Generate  $(\mathbf{x}_t, c_{i_t})$  from  $C_t$ 
13:   end if
14:   Generate  $\mathbf{s}_t(\mathbf{x}_t, c_{i_t})$  from  $\mathcal{S}(\mathbf{x}_t, c_{i_t})$ 
15:    $y_t \leftarrow f(\mathbf{s}_t(\mathbf{x}_t, c_{i_t})) + \varrho_t$ 
16:    $t \leftarrow t + 1$ 
17: end while
18:  $\widehat{H} \leftarrow \widehat{H}_{t-1}, \widehat{L} \leftarrow \widehat{L}_{t-1}$ 
```

we define that $\Phi(\sqrt{\sigma_t^2(\mathbf{s}^*) + \sigma^2} |k_t(\mathbf{a}, \mathbf{s}^*)|^{-1} c_t^+(\mathbf{a} | \mathbf{s}^*))$ is equal to one if $c_t^+(\mathbf{a} | \mathbf{s}^*) > 0$, and otherwise 0. Similarly, when $k_t(\mathbf{a}, \mathbf{s}^*) = 0$, we also define that $\Phi(\sqrt{\sigma_t^2(\mathbf{s}^*) + \sigma^2} |k_t(\mathbf{a}, \mathbf{s}^*)|^{-1} c_t^-(\mathbf{a} | \mathbf{s}^*))$ is equal to one if $c_t^-(\mathbf{a} | \mathbf{s}^*) > 0$, and otherwise 0.

The proof is given in Appendix A. Moreover, the details of approximation for the integral in (3.2) are given in Appendix B.

3.2.2. The randomized strategy

In the proposed algorithm we select the pair (\mathbf{x}, c_i) stochastically. Let $\mathcal{C} = \{(\mathbf{x}, c_i) \mid \mathbf{x} \in \Omega, i \in [k]\}$, C_t be a discrete random variable whose range is \mathcal{C} , and $\kappa_i = P(C_t = (\mathbf{x}, c_i))$ be a probability mass function of C_t , where $0 < \kappa_i < 1$ and $|\Omega| \sum_{i=1}^k \kappa_i = 1$.

3.2.3. Proposed algorithm

Using the results so far, we propose an algorithm for LSE with cost-dependent input uncertainty as follows. For each trial, (\mathbf{x}, c_i) is chosen by maximizing $a_t(\mathbf{x}, c_i)$ with probability $1 - p_t$, and otherwise (\mathbf{x}, c_i) is chosen based on the randomized strategy. The pseudo code of the proposed algorithm is given in Algorithm 1, where $\mathcal{B}(p_t)$ is Bernoulli distribution which takes 1 with probability p_t .

4. Extensions

In this section, we give two extensions of the proposed method. The first is an extension to the situation where error variances also change depending on costs, and the second covers the case where input distributions are unknown.

4.1. Cost-dependent error variances

Let $c_1^{(\text{out})}, \dots, c_{k^*}^{(\text{out})}$ be costs with $0 < c_1^{(\text{out})} < \dots < c_{k^*}^{(\text{out})}$. For each $c_o^{(\text{out})}$, $o \in [k^*]$ and $\mathbf{s} \in D$, a value of f can be observed as $y^{(o)} = f(\mathbf{s}) + \varrho^{(o)}$, where $\varrho^{(o)}$ is an independent Gaussian noise distributed as $\mathcal{N}(0, \sigma^{(o)2})$. Then, the posterior mean, variance and covariance of f after adding the data set $\{(\mathbf{s}_j(\mathbf{x}_j, c_{i_j}), y_j^{(o_j)})\}_{j=1}^t$ are given by

$$\mu_t(\mathbf{x}) = \mathbf{k}_t(\mathbf{x})^\top \bar{\mathbf{C}}_t^{-1} \mathbf{y}_t, \sigma_t^2(\mathbf{x}) = k_t(\mathbf{x}, \mathbf{x}), k_t(\mathbf{x}, \mathbf{x}') = k(\mathbf{x}, \mathbf{x}') - \mathbf{k}_t(\mathbf{x})^\top \bar{\mathbf{C}}_t^{-1} \mathbf{k}_t(\mathbf{x}'),$$

where $\bar{\mathbf{C}}_t = \mathbf{K}_t + \text{diag}(\sigma^{(o_1)^2}, \dots, \sigma^{(o_t)^2})$. In this case, if observation costs for the input point $\mathbf{x} \in \Omega$ and the function value are respectively c_i and $c_o^{(\text{out})}$, then the integral $a_t(\mathbf{x}, c_i, c_o^{(\text{out})})$ of the expected classification improvement per unit cost can be defined in the same way as (3.2). Therefore, similarly to Lemma 3.1, $a_t(\mathbf{x}, c_i, c_o^{(\text{out})})$ can be written as follows:

Lemma 4.1. The acquisition function $a_t(\mathbf{x}, c_i, c_o^{(\text{out})})$ can be written as

$$\begin{aligned} & a_t(\mathbf{x}, c_i, c_o^{(\text{out})}) \\ &= (c_i + c_o^{(\text{out})})^{-1} \int \left[\sum_{\mathbf{a} \in \Omega} \left\{ \Phi \left(\frac{\sqrt{\sigma_t^2(\mathbf{s}^*) + \sigma^{(o)^2}}}{|k_t(\mathbf{a}, \mathbf{s}^*)|} c_t^+(\mathbf{a}|\mathbf{s}^*) \right) + \Phi \left(\frac{\sqrt{\sigma_t^2(\mathbf{s}^*) + \sigma^{(o)^2}}}{|k_t(\mathbf{a}, \mathbf{s}^*)|} c_t^-(\mathbf{a}|\mathbf{s}^*) \right) \right\} - |HL_t| \right] \\ & \quad g(\mathbf{s}^*|\theta_{\mathbf{x}}^{(c_i)}) d\mathbf{s}^*. \end{aligned} \tag{4.1}$$

Here, if $k_t(\mathbf{a}, \mathbf{s}^*) = 0$, $\Phi(\cdot)$ is defined as in Lemma 3.1.

This lemma can be proven by following the same line of the proof of Lemma 3.1.

4.2. Unknown input distributions

Here, we discuss the case where the density function $g(\mathbf{s}|\theta_{\mathbf{x}}^{(c_i)})$ is unknown. In this case, it is necessary to estimate it. One natural approach is to estimate an unknown parameter $\theta_{\mathbf{x}}^{(c_i)}$ under the assumption that the density function has the known form $g(\mathbf{s}|\theta_{\mathbf{x}}^{(c_i)})$. However, if we assume a different $\theta_{\mathbf{x}}^{(c_i)}$ for each point $\mathbf{x} \in \Omega$ (and c_i), it is difficult to estimate the parameters. For this reason, we assume that $\theta_{\mathbf{x}}^{(c_i)}$ can be expressed as $\theta_{\mathbf{x}}^{(c_i)} = (\tilde{\theta}_{\mathbf{x}}^{(c_i)}, \xi^{(c_i)})$, where $\tilde{\theta}_{\mathbf{x}}^{(c_i)}$ is known, and $\xi^{(c_i)}$ is unknown. Then, by assuming a prior distribution $\pi(\xi^{(c_i)})$ for $\xi^{(c_i)}$, we can compute the posterior distribution $\pi_t(\xi^{(c_i)})$ after adding the data $\{(\mathbf{s}_j(\mathbf{x}_j, c_{i,j}), y_j)\}_{j=1}^t$. Therefore, by using this, $g(\mathbf{s}|\theta_{\mathbf{x}}^{(c_i)})$ can be estimated as

$$g_t(\mathbf{s}|\theta_{\mathbf{x}}^{(c_i)}) = \int g(\mathbf{s}|\theta_{\mathbf{x}}^{(c_i)}) \pi_t(\xi^{(c_i)}) d\xi^{(c_i)}.$$

5. Theoretical results

In this section, we give two theorems about accuracy and convergence of the proposed algorithm. First, for each $\mathbf{x} \in \Omega$, we define a misspecification loss at the end of the algorithm as

$$e_h(\mathbf{x}) = \begin{cases} \max\{0, f(\mathbf{x}) - h\} & \text{if } \mathbf{x} \in \hat{L} \\ \max\{0, h - f(\mathbf{x})\} & \text{if } \mathbf{x} \in \hat{H} \end{cases}.$$

Then, the following theorem holds:

Theorem 5.1. For any $h \in \mathbb{R}$, $\delta \in (0, 1)$ and $\epsilon > 0$, if $\beta = 2 \log(|\Omega|\delta^{-1})$, then with probability at least $1 - \delta$, the misspecification loss at the end of Algorithm 1 is less than ϵ . That is, the following inequality holds:

$$\mathbb{P} \left(\max_{\mathbf{x} \in \Omega} e_h(\mathbf{x}) \leq \epsilon \right) \geq 1 - \delta.$$

The proof is given in Appendix C. Next, we consider the convergence of Algorithm 1. Recall that inputs have uncertainty in this paper unlike the usual BO setting. Therefore, the desired input point may be greatly different from the actually input point. Furthermore, this can happen every trial. This implies that a probabilistic evaluation is needed when we analyze the convergence of the algorithm. Hence, in order to make a probabilistic evaluation, we assume the following three conditions:

(A1) Probabilities $\{p_t\}_{t \in \mathbb{N}}$ satisfy $\sum_{t=1}^{\infty} p_t = \infty$.

(A2) For any $\mathbf{x} \in \Omega$ and $\eta > 0$, there exists $\mathbf{x}' \in \Omega$ and c_i such that $\mathbb{P}(\mathcal{S}(\mathbf{x}', c_i) \in \mathcal{N}(\mathbf{x}; \eta)) > 0$, where $\mathcal{N}(\mathbf{x}; \eta) \equiv \{\mathbf{a} \in D \mid \|\mathbf{a} - \mathbf{x}\| < \eta\}$.

(A3) For any $\mathbf{x} \in \Omega$, the kernel function k is continuous at (\mathbf{x}, \mathbf{x}) .

The condition (A1) holds when each p_t is larger than a positive constant c . Moreover, (A1) holds even if $p_t = o(t^{-1})$. The condition (A2) requires the existence of an input $\mathbf{x}' \in \Omega$ and a cost c_i that can take a value around $\mathbf{x} \in \Omega$. The condition (A3) only requires that k is continuous on $\{(\mathbf{x}, \mathbf{x}) \mid \mathbf{x} \in \Omega\}$, not $D \times D$. Thus, (A1)–(A3) are mild conditions. Then, the following theorem holds:

Theorem 5.2. Assume that (A1) – (A3) hold. Then, for any $h \in \mathbb{R}$, $\epsilon > 0$ and $\beta > 0$, with probability 1, the following holds for any $\mathbf{x} \in \Omega$:

$$\sigma_t^2(\mathbf{x}) \rightarrow 0 \quad (\text{as } t \rightarrow \infty).$$

Furthermore, with probability 1, the number of evaluations of points required to complete Algorithm 1 is finite.

The proof is given in Appendix D.

6. Numerical experiments

In this section, we confirm the usefulness of the proposed method through numerical experiments using synthetic and real data. The results of numerical experiments not included in this main text are given in Appendix E.

6.1. Synthetic experiments

In this subsection, we compare the proposed method with some existing methods using synthetic functions. Hereafter, for simplicity, we used $p_t = 0$.

6.1.1. Sinusoidal function

We considered the function $f(x_1, x_2) = \sin(10x_1) + \cos(4x_2) - \cos(3x_1x_2)$ which was used in [4] as a true function, and defined the grid point obtained by uniformly cutting the region $[0, 1] \times [0, 2]$ into 30×60 as Ω . In addition, we used the Gaussian kernel with $\sigma_f^2 = e^2$ and $L = 2e^{-3}$. Moreover, we set $\sigma^2 = e^{-2}$, $h = 1$, $\epsilon = 10^{-12}$ and $\beta^{1/2} = 1.96$.

In this experiment, we considered three costs $c_1 = 1$, $c_2 = 2$ and $c_3 = 3$. For each c_i and $\mathbf{x} = (x_1, x_2)^\top \in \Omega$, we defined the input distribution as

$$\mathbf{S}(\mathbf{x}, c_i) = \mathbf{x} + (G_{[0,1-x_1]}(\zeta^{(i)}, 1), G_{[0,2-x_2]}(\zeta^{(i)}, 1))^\top.$$

Here, $G_{[0,a]}(b, c)$ is a gamma distribution with parameters b and c which is restricted on the interval $[0, a]$. We assumed that $G_{[0,1-x_1]}(\zeta^{(i)}, 1)$ and $G_{[0,2-x_2]}(\zeta^{(i)}, 1)$ are independent. Furthermore, we used that $\zeta^{(1)} = 4$ and $\zeta^{(2)} = 1$, $\zeta^{(3)} = 0.01$.

Then, we compared the following seven methods ($i = 1, 2, 3$):

(Cost i) Always take input points using cost i . In addition, the acquisition function is calculated without integrating against input distribution.

(Cost i EX) Always take input points using cost i . In addition, the acquisition function is calculated with integrating against input distribution.

(Cost123EX) All costs are allowed, and $a_t(\mathbf{x}, c_i)$ is used as the acquisition function.

In order to calculate integrals, we used the Monte Carlo approximation (details are given in (B.2)). Moreover, to estimate the discrete distribution, $\tilde{\mathbf{S}}(\mathbf{x}, c_i)$ was estimated by generating independent samples from each $\mathbf{S}(\mathbf{x}, c_i)$ thousand times. Under this setting, one initial point was taken at random, and points were acquired until the total cost reached 150. The classification performance was evaluated using the following accuracy:

$$\text{Accuracy} = \frac{|H \cap (H_t \setminus L_t)| + |L \cap (L_t \setminus H_t)|}{|\Omega|}.$$

The average obtained by 20 Monte Carlo simulations is given in Figure 2. From the leftmost figure of Figure 2, we can confirm that it is important to integrate against the input distribution when calculating the acquisition function. We can also see that the red line (proposed method) that appropriately selects the cost at each trial achieves the highest accuracy. Next, we compared with the following existing methods:

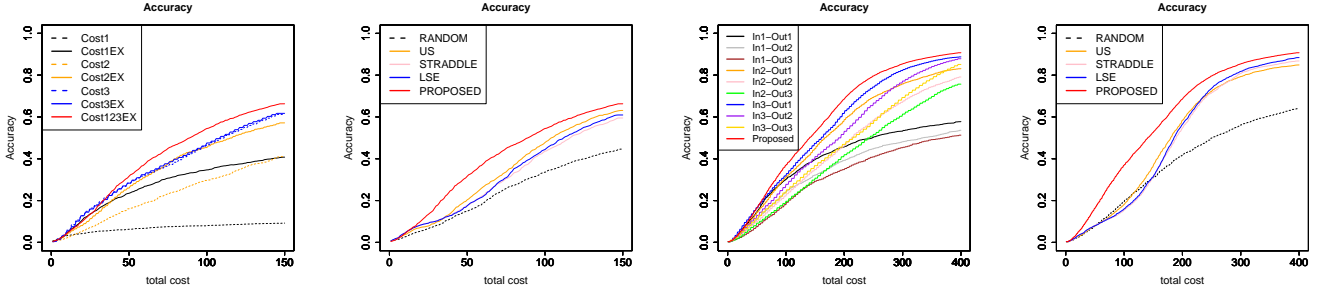


Figure 2: Average accuracy based on 20 Monte Carlo simulations in the Sinusoidal function (first and second columns) and Rosenbrock function (third and fourth columns). The first figure shows the influence of integration against the input distribution and that of cost in evaluating the input point. The second figure shows the result of comparison with existing methods. The third figure shows the influence of integration against the input distribution and that of costs for evaluating the input point and evaluating the function value. The fourth figure shows the result of comparison with existing methods.

(RANDOM) Perform random sampling.

(US) Perform uncertainty sampling, i.e., we select the input point with the largest posterior variance.

(STRADDLE) Perform straddle strategy [4], where we used $\beta_t^{1/2} = 1.96$.

(LSE) Perform LSE strategy [8], where we used $\beta_t^{1/2} = 1.96$.

In this experiment, US, STRADDLE, and LSE were tested in advance in the same way as the proposed method with a total of seven types including the presence or absence of integration against the input distribution and the presence or absence of cost sensitive. Among them, the one with the highest accuracy is used for comparison. Similarly, for RANDOM, we tried a total of four types with or without cost sensitive and used the best results for comparison. From the second from the left in Figure 2, we can confirm that the proposed method has higher accuracy than other existing methods.

6.1.2. Two-dimensional Rosenbrock function with cost dependent noise variance

Here, we considered the 2-dimensional Rosenbrock function (reduced to 1/100 and moved) $f(x_1, x_2) = (x_2 - x_1^2)^2 + (1 - x_1)^2/100 - 5$ as the true function, and defined the grid point obtained by uniformly cutting the region $[-2, 2] \times [-1, 3]$ into 40×40 as Ω . Furthermore, we used the Gaussian kernel with $\sigma_f^2 = 64$ and $L = 0.5$. In addition, we set $\sigma^2 = 0.25$, $h = 0$, $\epsilon = 10^{-12}$ and $\beta^{1/2} = 1.96$. Similarly in this experiment, we considered three costs $c_1 = 1$, $c_2 = 2$ and $c_3 = 3$. Moreover, for each c_i and $\mathbf{x} = (x_1, x_2)^\top \in \Omega$, we assumed that

$$\mathbf{S}(\mathbf{x}, c_i) = \mathbf{x} + (G_{[0,2-x_1]}(\zeta^{(i)}, 1), G_{[0,3-x_2]}(\zeta^{(i)}, 1))^\top,$$

where $G_{[0,2-x_1]}(\zeta^{(i)}, 1)$ and $G_{[0,3-x_2]}(\zeta^{(i)}, 1)$ are independent. Furthermore, we used $\zeta^{(1)} = 4$, $\zeta^{(2)} = 1$, $\zeta^{(3)} = 0.01$. Moreover, we consider the situation where the noise in the output also changes according to the cost. In this experiment, we considered three output costs $c_1^{(\text{out})} = 1$, $c_2^{(\text{out})} = 2$ and $c_3^{(\text{out})} = 3$, and then we defined $\varrho^{(j)} \sim \mathcal{N}(0, \sigma^{(j)2})$ as the error distribution, where $j \in \{1, 2, 3\}$. Furthermore, we set that $\sigma^{(1)2} = 0.5$, $\sigma^{(2)2} = 0.3$ and $\sigma^{(3)2} = 0.1$. Then, we compared the following ten methods ($i, j \in \{1, 2, 3\}$):

(In i -Out j) Take the input point using the cost i and observe the function value using the cost j . In addition, in the calculation of the acquisition function, integration is performed against the input distribution.

(PROPOSED) All costs are allowed, and the acquisition function is calculated by (4.1).

Under this setting, we performed the similar experiment as in sinusoidal function until the total cost reached 400. From the two figures on the right in Figure 2, even when the output has the cost-dependent error variance, we can see that the proposed method has higher accuracy than the other methods.

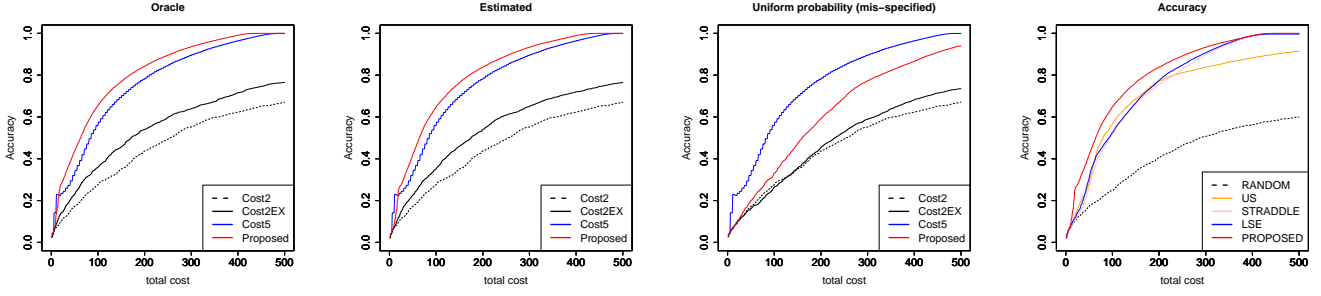


Figure 3: Average accuracy based on 50 Monte Carlo simulations in the Rhodopsin Data Set. The first, second and third figures show the influences of cost-sensitive and input distribution estimation. The fourth figure shows the result of comparison with existing methods.

6.2. Real data experiment

We conducted a real data experiment using the Rhodopsin-family protein data set provided by [9]. Rhodopsin-family proteins have a function to absorb a light with certain wavelength, and this function is effectively used in optogenetics [5]. The goal of this experiment is to estimate the level set in the protein feature space in which the absorption wavelength is sufficiently large for optogenetics usage. This dataset contains 677 proteins, where each protein i has a 210-dimensional amino acids sequence vector and a scalar absorption wavelength output. We first constructed a Bayesian linear model using amino acid sequences, modeled the relationship between amino acid sequences and absorption wavelengths, and conducted experiments using this model as the oracle model. In the experiment, 400 pseudo-proteins were constructed by changing the amino acids of the 150th and 200th residues of the 338th rhodopsin, which has an intermediate absorption wavelength, to 20 different amino acids. The absorption wavelength of this protein was determined based on the constructed prediction model, and this was set as $y_{i,j}$, $i, j \in [20]$, where the average of $y_{i,j}$ was standardized to be 0. Here, (i, j) in $y_{i,j}$ means that the 150th residue is changed to the i th amino acid and the 200th residue is changed to the j th amino acid. In addition, the i th amino acid means the i th amino acid when the one-letter code of the amino acid is arranged in alphabetical order. As an input corresponding to the response variable $y_{i,j}$, we used a 42-dimensional feature vector $\mathbf{x}_{i,j} = (\mathbf{x}_i^\top, \mathbf{x}_j^\top)^\top$ consisting of amino acid features (e.g., volume, molecular weight), where $\mathbf{x}_i, \mathbf{x}_j \in \mathbb{R}^{21}$.

We assumed that the true output value $y_{i,j}$ can be observed without any noise. However, for convenience of calculation, we used $\sigma^2 = 10^{-6}$. Furthermore, we defined the input domain as $\Omega = \{\mathbf{x}_{i,j} \mid i, j \in [20]\}$. We used the Gaussian kernel with $\sigma_f^2 = 10$ and $L = 200$. In addition, we set $h = 0$, $\epsilon = 10^{-12}$ and $\beta^{1/2} = 3$. In this experiment, we considered two costs $c_1 = 2$ and $c_2 = 5$. Then, for input distributions, we assumed the following synthetic discrete distribution $\mathbf{S}(\mathbf{x}_u, c_k)$:

$$\begin{aligned} \mathbb{P}(\mathbf{S}(\mathbf{x}_u, c_1) = \mathbf{x}_v) &= 0.8/3 \quad (v = 7, 9, 15), \\ \mathbb{P}(\mathbf{S}(\mathbf{x}_u, c_1) = \mathbf{x}_v) &= 0.1/2 \quad (v = 3, 4), \\ \mathbb{P}(\mathbf{S}(\mathbf{x}_u, c_1) = \mathbf{x}_v) &= 0.1/15 \quad (v \in [20] \setminus \{3, 4, 7, 9, 15\}), \\ \mathbb{P}(\mathbf{S}(\mathbf{x}_u, c_2) = \mathbf{x}_u) &= 1. \end{aligned}$$

In other words, $\mathbf{S}(\mathbf{x}_u, c_2)$ takes \mathbf{x}_u with probability 1. Moreover, $\mathbf{S}(\mathbf{x}_u, c_1)$ is a random mutation where the probability which takes each acidic, basic and neutral amino acid are 0.8/3, 0.1/2 and 0.1/15, respectively. Therefore, it is a mutation that easily becomes acidic amino acids. Based on these, we defined the input distributions as

$$\begin{aligned} \mathbf{S}(\mathbf{x}_{u,v}, c_1) &= (\mathbf{S}(\mathbf{x}_u, c_1), \mathbf{S}(\mathbf{x}_v, c_1))^\top, \\ \mathbf{S}(\mathbf{x}_{u,v}, c_1) &= (\mathbf{S}(\mathbf{x}_u, c_1), \mathbf{x}_v)^\top \quad (\text{if there exists } y_{\cdot,v}), \\ \mathbf{S}(\mathbf{x}_{u,v}, c_1) &= (\mathbf{x}_u, \mathbf{S}(\mathbf{x}_v, c_1))^\top \quad (\text{if there exists } y_{u,\cdot}). \end{aligned}$$

Similarly, we defined

$$\begin{aligned} \mathbf{S}(\mathbf{x}_{u,v}, 2c_2) &= (\mathbf{x}_u, \mathbf{x}_v)^\top \quad (\text{if there are no } y_{u,\cdot}, y_{\cdot,v}), \\ \mathbf{S}(\mathbf{x}_{u,v}, c_2) &= (\mathbf{x}_u, \mathbf{x}_v)^\top \quad (\text{if there exists } y_{\cdot,v} \text{ or } y_{u,\cdot}). \end{aligned}$$

Under this setting, we considered the following three cases for $\mathcal{S}(\mathbf{x}_u, c_1)$: 1) the true distribution is known. 2) when estimating using categorical distribution and using Dirichlet distribution whose parameter is $\boldsymbol{\alpha} = (0.75, 0.5, 3.75)^\top$ as prior distribution. 3) when the discrete uniform distribution is used without estimation, i.e., the distribution is mis-specified. Then, we performed the similar experiment as in sinusoidal function until the total cost reached 500. The average obtained by 50 Monte Carlo simulations is given in Figure 3. From Figure 3, we can confirm that the proposed method has higher accuracy than except the mis-specified case. Moreover, from the first and second figures in Figure 3, even if the distribution is unknown, it can be confirmed that its performance is almost the same as oracle by estimating distribution parameters under the assumption that the true distribution form is known.

7. Conclusion

In this paper, we proposed a new active learning method for LSE under cost-dependent input uncertainty. The acquisition function in the proposed method is based on the integral of the expected increase in classification per unit cost. The usefulness of the proposed method was confirmed through both numerical experiments and theoretical analysis.

Acknowledgments

This work was supported by MEXT KAKENHI to I.T. (16H06538, 17H00758) and M.K. (16H06538, 17H04694); from JST CREST awarded to I.T. (JPMJCR1302, JPMJCR1502) and PRESTO awarded to M.K. (JPMJPR15N2); from the MI2I project of the Support Program for Starting Up Innovation Hub from JST awarded to I.T., and M.K.; and from RIKEN Center for AIP awarded to I.T.

References

- [1] Justin J Beland and Prasanth B Nair. Bayesian optimization under uncertainty. In *NIPS BayesOpt 2017 workshop*, 2017.
- [2] Christopher M Bishop. *Pattern recognition and machine learning*. springer, 2006.
- [3] Ilija Bogunovic, Jonathan Scarlett, Andreas Krause, and Volkan Cevher. Truncated variance reduction: A unified approach to bayesian optimization and level-set estimation. In D. D. Lee, M. Sugiyama, U. V. Luxburg, I. Guyon, and R. Garnett, editors, *Advances in Neural Information Processing Systems 29*, pages 1507–1515. Curran Associates, Inc., 2016.
- [4] Brent Bryan, Robert C Nichol, Christopher R Genovese, Jeff Schneider, Christopher J Miller, and Larry Wasserman. Active learning for identifying function threshold boundaries. In *Advances in neural information processing systems*, pages 163–170, 2006.
- [5] Karl Deisseroth. Optogenetics: 10 years of microbial opsins in neuroscience. *Nature neuroscience*, 18(9):1213–1225, 2015.
- [6] Alexandra Gessner, Javier Gonzalez, and Maren Mahsereci. Active multi-information source bayesian quadrature. In *Proceedings of the Thirty-Fifth Conference on Uncertainty in Artificial Intelligence, UAI 2019, Tel Aviv, Israel, July 22-25, 2019*, page 245, 2019.
- [7] Agathe Girard, Carl Edward Rasmussen, Joaquin Quiñonero Candela, and Roderick Murray-Smith. Gaussian process priors with uncertain inputs application to multiple-step ahead time series forecasting. In S. Becker, S. Thrun, and K. Obermayer, editors, *Advances in Neural Information Processing Systems 15*, pages 545–552. MIT Press, 2003.
- [8] Alkis Gotovos, Nathalie Casati, Gregory Hitz, and Andreas Krause. Active learning for level set estimation. In *Proceedings of the Twenty-Third International Joint Conference on Artificial Intelligence*, pages 1344–1350, 2013.
- [9] Masayuki Karasuyama, Keiichi Inoue, Hideki Kandori, and Ichiro Takeuchi. Toward machine learning-based data-driven functional protein studies: Understanding colour tuning rules and predicting the absorption wavelengths of microbial rhodopsins. *bioRxiv*, page 226118, 2017.

- [10] Anthony O’Hagan. Bayes–hermite quadrature. *Journal of statistical planning and inference*, 29(3):245–260, 1991.
- [11] Rafael Oliveira, Lionel Ott, and Fabio Ramos. Bayesian optimisation under uncertain inputs. In Kamalika Chaudhuri and Masashi Sugiyama, editors, *Proceedings of Machine Learning Research*, volume 89 of *Proceedings of Machine Learning Research*, pages 1177–1184. PMLR, 16–18 Apr 2019.
- [12] Matthias Poloczek, Jialei Wang, and Peter Frazier. Multi-information source optimization. In I. Guyon, U. V. Luxburg, S. Bengio, H. Wallach, R. Fergus, S. Vishwanathan, and R. Garnett, editors, *Advances in Neural Information Processing Systems 30*, pages 4288–4298. Curran Associates, Inc., 2017.
- [13] Carl Edward Rasmussen and Christopher K. I. Williams. *Gaussian Processes for Machine Learning (Adaptive Computation and Machine Learning)*. The MIT Press, 2005.
- [14] James R Schott. *Matrix analysis for statistics*. John Wiley & Sons, 2016.
- [15] Warren Scott, Peter Frazier, and Warren Powell. The correlated knowledge gradient for simulation optimization of continuous parameters using gaussian process regression. *SIAM Journal on Optimization*, 21(3):996–1026, 2011.
- [16] Burr Settles. Active learning literature survey. Computer Sciences Technical Report 1648, University of Wisconsin–Madison, 2009.
- [17] Bobak Shahriari, Kevin Swersky, Ziyu Wang, Ryan P Adams, and Nando De Freitas. Taking the human out of the loop: A review of bayesian optimization. *Proceedings of the IEEE*, 104(1):148–175, 2016.
- [18] Jun Shao. *Mathematical Statistics*. Springer-Verlag New York Inc, 2nd edition, 2003.
- [19] Shubhanshu Shekhar and Tara Javidi. Multiscale gaussian process level set estimation. In Kamalika Chaudhuri and Masashi Sugiyama, editors, *Proceedings of Machine Learning Research*, volume 89 of *Proceedings of Machine Learning Research*, pages 3283–3291. PMLR, 16–18 Apr 2019.
- [20] Jialin Song, Yuxin Chen, and Yisong Yue. A general framework for multi-fidelity bayesian optimization with gaussian processes. In Kamalika Chaudhuri and Masashi Sugiyama, editors, *Proceedings of Machine Learning Research*, volume 89 of *Proceedings of Machine Learning Research*, pages 3158–3167. PMLR, 16–18 Apr 2019.
- [21] Niranjana Srinivas, Andreas Krause, Sham Kakade, and Matthias Seeger. Gaussian process optimization in the bandit setting: No regret and experimental design. In *Proceedings of the 27th International Conference on Machine Learning*, pages 1015–1022, 2010.
- [22] Yanan Sui, Alkis Gotovos, Joel Burdick, and Andreas Krause. Safe exploration for optimization with gaussian processes. In *International Conference on Machine Learning*, pages 997–1005, 2015.
- [23] Yanan Sui, Vincent Zhuang, Joel W. Burdick, and Yisong Yue. Stagewise safe bayesian optimization with gaussian processes. In *ICML*, volume 80 of *Proceedings of Machine Learning Research*, pages 4788–4796. PMLR, 2018.
- [24] Kevin Swersky, Jasper Snoek, and Ryan P Adams. Multi-task bayesian optimization. In C. J. C. Burges, L. Bottou, M. Welling, Z. Ghahramani, and K. Q. Weinberger, editors, *Advances in Neural Information Processing Systems 26*, pages 2004–2012. Curran Associates, Inc., 2013.
- [25] Matteo Turchetta, Felix Berkenkamp, and Andreas Krause. Safe exploration in finite markov decision processes with gaussian processes. In *Advances in Neural Information Processing Systems*, pages 4312–4320, 2016.
- [26] Akifumi Wachi, Yanan Sui, Yisong Yue, and Masahiro Ono. Safe exploration and optimization of constrained mdps using gaussian processes. In *AAAI*, pages 6548–6556. AAAI Press, 2018.
- [27] Xiaoyue Xi, Francois-Xavier Briol, and Mark Girolami. Bayesian quadrature for multiple related integrals. In *International Conference on Machine Learning*, pages 5369–5378, 2018.

[28] Andrea Zanette, Junzi Zhang, and Mykel J Kochenderfer. Robust super-level set estimation using gaussian processes. In *Joint European Conference on Machine Learning and Knowledge Discovery in Databases*, pages 276–291. Springer, 2018.

Appendix

A. Proof of Lemma 3.1

Proof. The proof is given in the same way as the proof of Lemma 2 in [28]. Let $h_t(y^*)$ be a probability density function of y^* at t th trial. Then, $\mathbb{E}_{y^*} [|H_{t+1}(\mathbf{s}^*, y^*) \cup L_{t+1}(\mathbf{s}^*, y^*)|]$ can be expressed as follows:

$$\begin{aligned}
& \mathbb{E}_{y^*} [|H_{t+1}(\mathbf{s}^*, y^*) \cup L_{t+1}(\mathbf{s}^*, y^*)|] \\
&= \mathbb{E}_{y^*} \left[\sum_{\mathbf{a} \in \Omega} \mathbb{1}\{\mu_t(\mathbf{a} | (\mathbf{s}^*, y^*)) - \beta^{1/2} \sigma_t(\mathbf{a} | \mathbf{s}^*) > h - \epsilon\} \right. \\
&\quad \left. + \sum_{\mathbf{a} \in \Omega} \mathbb{1}\{\mu_t(\mathbf{a} | (\mathbf{s}^*, y^*)) + \beta^{1/2} \sigma_t(\mathbf{a} | \mathbf{s}^*) < h + \epsilon\} \right] \\
&= \sum_{\mathbf{a} \in \Omega} \mathbb{E}_{y^*} [\mathbb{1}\{\mu_t(\mathbf{a} | (\mathbf{s}^*, y^*)) - \beta^{1/2} \sigma_t(\mathbf{a} | \mathbf{s}^*) > h - \epsilon\}] \\
&\quad + \sum_{\mathbf{a} \in \Omega} \mathbb{E}_{y^*} [\mathbb{1}\{\mu_t(\mathbf{a} | (\mathbf{s}^*, y^*)) + \beta^{1/2} \sigma_t(\mathbf{a} | \mathbf{s}^*) < h + \epsilon\}] \\
&= \sum_{\mathbf{a} \in \Omega} \mathbb{P}(\{\mu_t(\mathbf{a} | (\mathbf{s}^*, y^*)) - \beta^{1/2} \sigma_t(\mathbf{a} | \mathbf{s}^*) > h - \epsilon\}) \\
&\quad + \sum_{\mathbf{a} \in \Omega} \mathbb{P}(\{\mu_t(\mathbf{a} | (\mathbf{s}^*, y^*)) + \beta^{1/2} \sigma_t(\mathbf{a} | \mathbf{s}^*) < h + \epsilon\}) \\
&= \sum_{\mathbf{a} \in \Omega} \int_{-\infty}^{\infty} [\mathbb{1}\{\{\mu_t(\mathbf{a} | (\mathbf{s}^*, y^*)) - \beta^{1/2} \sigma_t(\mathbf{a} | \mathbf{s}^*) > h - \epsilon\}\}] h_t(y^*) dy^*, \\
&\quad + \mathbb{1}\{\{\mu_t(\mathbf{a} | (\mathbf{s}^*, y^*)) + \beta^{1/2} \sigma_t(\mathbf{a} | \mathbf{s}^*) < h + \epsilon\}\}] h_t(y^*) dy^*,
\end{aligned}$$

where $\mathbb{1}\{\cdot\}$ is an indicator function, and $\mu_t(\mathbf{a} | (\mathbf{s}^*, y^*))$ is the posterior mean of $f(\mathbf{a})$ after adding (\mathbf{s}^*, y^*) to $\{(\mathbf{s}_j(\mathbf{x}_j, c_{i_j}), y_j)\}_{j=1}^t$. Moreover, from basic properties of GP (see, e.g., [13]), $\mu_t(\mathbf{a} | (\mathbf{s}^*, y^*))$ and $\sigma_t^2(\mathbf{a} | \mathbf{s}^*)$ are given by

$$\begin{aligned}
\sigma_t^2(\mathbf{a} | \mathbf{s}^*) &= \sigma_t^2(\mathbf{a}) - \frac{k_t^2(\mathbf{a}, \mathbf{s}^*)}{\sigma_t^2(\mathbf{s}^*) + \sigma^2}, \\
\mu_t(\mathbf{a} | (\mathbf{s}^*, y^*)) &= \mu_t(\mathbf{a}) - \frac{k_t(\mathbf{a}, \mathbf{s}^*)}{\sigma_t^2(\mathbf{s}^*) + \sigma^2} (y^* - \mu_t(\mathbf{s}^*)).
\end{aligned}$$

Hence, by using these we have

$$\begin{aligned}
& \mu_t(\mathbf{a} | (\mathbf{s}^*, y^*)) - \beta^{1/2} \sigma_t(\mathbf{a} | \mathbf{s}^*) > h - \epsilon \\
&\Leftrightarrow \mu_t(\mathbf{a}) - \frac{k_t(\mathbf{a}, \mathbf{s}^*)}{\sigma_t^2(\mathbf{s}^*) + \sigma^2} (y^* - \mu_t(\mathbf{s}^*)) - \beta^{1/2} \sigma_t(\mathbf{a} | \mathbf{s}^*) > h - \epsilon \\
&\Leftrightarrow \frac{k_t(\mathbf{a}, \mathbf{s}^*)}{\sigma_t^2(\mathbf{s}^*) + \sigma^2} (y^* - \mu_t(\mathbf{s}^*)) < c_t^+(\mathbf{a} | \mathbf{s}^*).
\end{aligned}$$

Therefore, noting that $(y^* - \mu_t(\mathbf{s}^*)) / (\sigma_t^2(\mathbf{s}^*) + \sigma^2)^{1/2} \sim \mathcal{N}(0, 1)$, if $k_t(\mathbf{a}, \mathbf{s}^*) > 0$, the following holds:

$$\begin{aligned}
& \int_{-\infty}^{\infty} \mathbb{1}\{\{\mu_t(\mathbf{a} | (\mathbf{s}^*, y^*)) - \beta^{1/2} \sigma_t(\mathbf{a} | \mathbf{s}^*) > h - \epsilon\}\} h_t(y^*) dy^* \\
&= \int_{-\infty}^{\infty} \mathbb{1}\left\{\frac{y^* - \mu_t(\mathbf{s}^*)}{\sqrt{\sigma_t^2(\mathbf{s}^*) + \sigma^2}} < \frac{\sqrt{\sigma_t^2(\mathbf{s}^*) + \sigma^2}}{|k_t(\mathbf{a}, \mathbf{s}^*)|} c_t^+(\mathbf{a} | \mathbf{s}^*)\right\} h_t(y^*) dy^* \\
&= \int_{-\infty}^{\infty} \mathbb{1}\left\{z < \frac{\sqrt{\sigma_t^2(\mathbf{s}^*) + \sigma^2}}{|k_t(\mathbf{a}, \mathbf{s}^*)|} c_t^+(\mathbf{a} | \mathbf{s}^*)\right\} \phi(z) dz \\
&= \Phi\left(\frac{\sqrt{\sigma_t^2(\mathbf{s}^*) + \sigma^2}}{|k_t(\mathbf{a}, \mathbf{s}^*)|} \times (\mu_t(\mathbf{a}) - \beta^{1/2} \sigma_t(\mathbf{a} | \mathbf{s}^*) - h + \epsilon)\right).
\end{aligned}$$

Similarly, if $k_t(\mathbf{a}, \mathbf{s}^*) < 0$, it holds that

$$\begin{aligned}
& \int_{-\infty}^{\infty} \mathbb{1}\{\{\mu_t(\mathbf{a} | (\mathbf{s}^*, y^*)) - \beta^{1/2} \sigma_t(\mathbf{a} | \mathbf{s}^*) > h - \epsilon\}\} h_t(y^*) dy^* \\
&= \int_{-\infty}^{\infty} \mathbb{1}\left\{-\frac{y^* - \mu_t(\mathbf{s}^*)}{\sqrt{\sigma_t^2(\mathbf{s}^*) + \sigma^2}} < \frac{\sqrt{\sigma_t^2(\mathbf{s}^*) + \sigma^2}}{|k_t(\mathbf{a}, \mathbf{s}^*)|} c_t^+(\mathbf{a} | \mathbf{s}^*)\right\} h_t(y^*) dy^* \\
&= \int_{-\infty}^{\infty} \mathbb{1}\left\{-z < \frac{\sqrt{\sigma_t^2(\mathbf{s}^*) + \sigma^2}}{|k_t(\mathbf{a}, \mathbf{s}^*)|} c_t^+(\mathbf{a} | \mathbf{s}^*)\right\} \phi(z) dz \\
&= \int_{\infty}^{-\infty} \mathbb{1}\left\{z' < \frac{\sqrt{\sigma_t^2(\mathbf{s}^*) + \sigma^2}}{|k_t(\mathbf{a}, \mathbf{s}^*)|} c_t^+(\mathbf{a} | \mathbf{s}^*)\right\} \phi(-z') (-dz') \\
&= \int_{-\infty}^{\infty} \mathbb{1}\left\{z' < \frac{\sqrt{\sigma_t^2(\mathbf{s}^*) + \sigma^2}}{|k_t(\mathbf{a}, \mathbf{s}^*)|} c_t^+(\mathbf{a} | \mathbf{s}^*)\right\} \phi(z') dz' \\
&= \Phi\left(\frac{\sqrt{\sigma_t^2(\mathbf{s}^*) + \sigma^2}}{|k_t(\mathbf{a}, \mathbf{s}^*)|} c_t^+(\mathbf{a} | \mathbf{s}^*)\right).
\end{aligned}$$

Finally, if $k_t(\mathbf{a}, \mathbf{s}^*) = 0$, we obtain

$$\begin{aligned}
& \int_{-\infty}^{\infty} \mathbb{1}\{\{\mu_t(\mathbf{a} | (\mathbf{s}^*, y^*)) - \beta^{1/2} \sigma_t(\mathbf{a} | \mathbf{s}^*) > h - \epsilon\}\} h_t(y^*) dy^* \\
&= \int_{-\infty}^{\infty} \mathbb{1}\{\mu_t(\mathbf{a}) - \beta^{1/2} \sigma_t(\mathbf{a} | \mathbf{s}^*) - h + \epsilon > 0\} h_t(y^*) dy^* \\
&= \begin{cases} 1 & \text{if } \mu_t(\mathbf{a}) - \beta^{1/2} \sigma_t(\mathbf{a} | \mathbf{s}^*) - h + \epsilon > 0 \\ 0 & \text{if } \mu_t(\mathbf{a}) - \beta^{1/2} \sigma_t(\mathbf{a} | \mathbf{s}^*) - h + \epsilon \leq 0 \end{cases}.
\end{aligned}$$

By using the same argument, the following integral

$$\int_{-\infty}^{\infty} \mathbb{1}\{\{\mu_t(\mathbf{a} | (\mathbf{s}^*, y^*)) + \beta^{1/2} \sigma_t(\mathbf{a} | \mathbf{s}^*) < h + \epsilon\}\} h_t(y^*) dy^*$$

can be also calculated. □

B. Approximation of $a_t(\mathbf{x}, c_i)$

Since integral operation about $\mathbf{S}(\mathbf{x}, c_i)$ in $a_t(\mathbf{x}, c_i)$ is computationally expensive, we consider two approximations of $a_t(\mathbf{x}, c_i)$.

Let $\mathbf{s}^{(1)}(\mathbf{x}, c_i), \dots, \mathbf{s}^{(M)}(\mathbf{x}, c_i)$ be independent random variables from $\mathbf{S}(\mathbf{x}, c_i)$. Then, $a_t(\mathbf{x}, c_i)$ can be approximated as

$$\begin{aligned}
& a_t(\mathbf{x}, c_i) \\
&\approx c_i^{-1} M^{-1} \sum_{j=1}^M \left\{ \sum_{\mathbf{a} \in \Omega} \Phi\left(\frac{\sqrt{\sigma_t^2(\mathbf{s}^{(j)}(\mathbf{x}, c_i)) + \sigma^2}}{|k_t(\mathbf{a}, \mathbf{s}^{(j)}(\mathbf{x}, c_i))|} \times (\mu_t(\mathbf{a}) - \beta^{1/2} \sigma_t(\mathbf{a} | \mathbf{s}^{(j)}(\mathbf{x}, c_i)) - h + \epsilon)\right) \right. \\
&\quad \left. + \sum_{\mathbf{a} \in \Omega} \Phi\left(\frac{\sqrt{\sigma_t^2(\mathbf{s}^{(j)}(\mathbf{x}, c_i)) + \sigma^2}}{|k_t(\mathbf{a}, \mathbf{s}^{(j)}(\mathbf{x}, c_i))|} \times (-\mu_t(\mathbf{a}) - \beta^{1/2} \sigma_t(\mathbf{a} | \mathbf{s}^{(j)}(\mathbf{x}, c_i)) + h + \epsilon)\right) - |HL_t| \right\}. \tag{B.1}
\end{aligned}$$

However, in (B.1), it is necessary to compute the posterior variance for each $\mathbf{s}^{(j)}(\mathbf{x}, c_i)$. As the result, the computational cost of (B.1) is $\mathcal{O}(t^2|\Omega|M)$. Therefore, the total computational cost required for one trial is $\mathcal{O}(t^2k|\Omega|^2M)$ because it is necessary to compute for all $\mathbf{x} \in \Omega$ and $c_i, i \in [k]$.

As another choice, we can consider the following approximate distribution of $\mathbf{S}(\mathbf{x}, c_i)$. Let $[\mathbf{a}]_\Omega$ be an element of Ω which is the closest point to \mathbf{a} . Then, we define $[\mathbf{S}(\mathbf{x}, c_i)]_\Omega \equiv \tilde{\mathbf{S}}(\mathbf{x}, c_i)$. Note that $\tilde{\mathbf{S}}(\mathbf{x}, c_i)$ is the discrete random variable whose observed value is in Ω . Then, $a_t(\mathbf{x}, c_i)$ can be approximated by using $\tilde{\mathbf{S}}(\mathbf{x}, c_i)$ as

$$\begin{aligned} a_t(\mathbf{x}, c_i) &\approx c_i^{-1} \sum_{\mathbf{b} \in \Omega} \left\{ \sum_{\mathbf{a} \in \Omega} \Phi \left(\frac{\sqrt{\sigma_t^2(\mathbf{b}) + \sigma^2}}{|k_t(\mathbf{a}, \mathbf{b})|} \times (\mu_t(\mathbf{a}) - \beta^{1/2}\sigma_t(\mathbf{a}|\mathbf{b}) - h + \epsilon) \right) \right. \\ &\quad \left. + \sum_{\mathbf{a} \in \Omega} \Phi \left(\frac{\sqrt{\sigma_t^2(\mathbf{b}) + \sigma^2}}{|k_t(\mathbf{a}, \mathbf{b})|} \times (-\mu_t(\mathbf{a}) - \beta^{1/2}\sigma_t(\mathbf{a}|\mathbf{b}) + h + \epsilon) \right) - |HL_t| \right\} p_{\tilde{\mathbf{S}}(\mathbf{x}, c_i)}(\mathbf{b}), \end{aligned} \quad (\text{B.2})$$

where $p_{\tilde{\mathbf{S}}(\mathbf{x}, c_i)}(\mathbf{a}) \equiv \text{P}(\tilde{\mathbf{S}}(\mathbf{x}, c_i) = \mathbf{a})$ is the probability mass function of $\tilde{\mathbf{S}}(\mathbf{x}, c_i)$. Unlike (B.1), in (B.2), the calculation results in the braces $\{\}$ are same for all $\mathbf{x} \in \Omega$ and c_i . Thus, for the calculation in the braces $\{\}$, it is sufficient to calculate once for each $\mathbf{a} \in \Omega$ and $\mathbf{b} \in \Omega$, and its calculation cost is given by $\mathcal{O}(t^2|\Omega|^2)$. Moreover, the computational cost required to calculate $a_t(\mathbf{x}, c_i)$ is $\mathcal{O}(|\Omega|)$. Therefore, the total cost of calculating $a_t(\mathbf{x}, c_i)$ is given by $\mathcal{O}((t^2 + k)|\Omega|^2)$. This approximation is useful when $\tilde{\mathbf{S}}(\mathbf{x}, c_i)$ is a good approximation of $\mathbf{S}(\mathbf{x}, c_i)$.

C. Proof of Theorem 5.1

Proof. For any $t \geq 1$, the following inequality holds with probability at least $1 - |\Omega|e^{-\beta/2}$ (see, e.g., Lemma 5.1 in [21]):

$$|f(\mathbf{x}) - \mu_t(\mathbf{x})| \leq \beta^{1/2}\sigma_t(\mathbf{x}), \quad \forall \mathbf{x} \in \Omega. \quad (\text{C.1})$$

Thus, by letting $\beta = 2 \log(|\Omega|\delta^{-1})$, (C.1) holds with probability at least $1 - \delta$. In addition, let T be t at the end of the algorithm. Then, with probability at least $1 - \delta$, it holds that

$$f(\mathbf{x}) \in Q_T(\mathbf{x}), \quad \forall \mathbf{x} \in \Omega. \quad (\text{C.2})$$

Hence, from (C.2) and (3.1) we get Theorem 5.1 \square

D. Proof of Theorem 5.2

First, we define several notations. For each $t \geq 1$ and $\mathbf{x} \in \Omega$, define

$$\zeta_t^2(\mathbf{x}) = k(\mathbf{x}, \mathbf{x}) - (k(\mathbf{x}, \mathbf{x})\mathbf{1}_t)^\top (k(\mathbf{x}, \mathbf{x})\mathbf{1}_t\mathbf{1}_t^\top + \sigma^2\mathbf{I}_t)^{-1} (k(\mathbf{x}, \mathbf{x})\mathbf{1}_t). \quad (\text{D.1})$$

Here, $\mathbf{1}_t$ is a t -dimensional vector where every element is equal to one. Hence, $\zeta_t^2(\mathbf{x})$ is the posterior variance of $f(\mathbf{x})$ when \mathbf{x} is chosen t times. Next, let E be an event, and let $\mathbf{1}_E$ be an indicator function which takes one if E holds and zero otherwise. Furthermore, for each $t \geq 1$, $\mathbf{x} \in \Omega$, and cost c_i , define

$$E_t(\mathbf{x}, c_i) = \{(\mathbf{x}_t, c_{i_t}) = (\mathbf{x}, c_i)\}. \quad (\text{D.2})$$

Note that $E_t(\mathbf{x}, c_i)$ is an event where \mathbf{x} is chosen using the cost c_i at t th trial. Next, for each (\mathbf{x}, c_i) , suppose that $\mathbf{W}_1(\mathbf{x}, c_i), \mathbf{W}_2(\mathbf{x}, c_i), \dots$ are random variables where $\mathbf{W}_1(\mathbf{x}, c_i), \mathbf{W}_2(\mathbf{x}, c_i), \dots \sim \text{i.i.d. } \mathbf{S}(\mathbf{x}, c_i)$. Moreover, for any $t \geq 1$, let \mathbf{A}_t be an input random variable at t th trial. Thus, \mathbf{A}_t can be expressed as

$$\mathbf{A}_t = \sum_{i=1}^k \sum_{\mathbf{x} \in \Omega} \mathbf{1}_{E_t(\mathbf{x}, c_i)} \mathbf{W}_t(\mathbf{x}, c_i). \quad (\text{D.3})$$

Finally, for each $t \geq 1$ and $\mathbf{x} \in \Omega$, define

$$\hat{\sigma}_t^2(\mathbf{x}) = k(\mathbf{x}, \mathbf{x}) - \hat{\mathbf{k}}_t(\mathbf{x})^\top (\hat{\mathbf{K}}_t + \sigma^2\mathbf{I}_t)^{-1} \hat{\mathbf{k}}_t(\mathbf{x}), \quad (\text{D.4})$$

where $\hat{\mathbf{k}}_t(\mathbf{x})$ is a t -dimensional vector whose j th element is $k(\mathbf{A}_j, \mathbf{x})$, and $\hat{\mathbf{K}}_t$ is a $t \times t$ matrix whose (u, v) element is $k(\mathbf{A}_u, \mathbf{A}_v)$. Note that $\sigma_t^2(\mathbf{x})$ is an observed value of the random variable $\hat{\sigma}_t^2(\mathbf{x})$. Hence, in order to prove the first half of Theorem 5.2, it is necessary to show that

$$\hat{\sigma}_t^2(\mathbf{x}) \xrightarrow{\text{a.s.}} 0, \quad (\text{D.5})$$

where (D.5) means that $\hat{\sigma}_t^2(\mathbf{x})$ converges to zero almost surely. The equation (D.5) can be proven by showing the following three facts:

(Fact1) For any $\mathbf{x} \in \Omega$, it holds that

$$\lim_{t \rightarrow \infty} \zeta_t^2(\mathbf{x}) = 0. \quad (\text{D.6})$$

(Fact2) For any $\mathbf{x} \in \Omega$, $\hat{\sigma}_t^2(\mathbf{x})$ converges in probability to zero (i.e., $\hat{\sigma}_t^2(\mathbf{x}) \xrightarrow{\text{P}} 0$).

(Fact3) For any $\mathbf{x} \in \Omega$, $\hat{\sigma}_t^2(\mathbf{x})$ converges to zero almost surely (i.e., $\hat{\sigma}_t^2(\mathbf{x}) \xrightarrow{\text{a.s.}} 0$).

First, we prove (Fact1).

Proof. Let \mathbf{H} be a $t \times t$ non-singular matrix. Then, for any t -dimensional vector \mathbf{a} and \mathbf{b} where $\mathbf{H} + \mathbf{a}\mathbf{b}^\top$ is a non-singular matrix, the following holds (see, e.g., [14]):

$$(\mathbf{H} + \mathbf{a}\mathbf{b}^\top)^{-1} = \mathbf{H}^{-1} - \frac{\mathbf{H}^{-1}\mathbf{a}\mathbf{b}^\top\mathbf{H}^{-1}}{1 + \mathbf{b}^\top\mathbf{H}^{-1}\mathbf{a}}. \quad (\text{D.7})$$

Thus, by letting $\mathbf{H} = \sigma^2\mathbf{I}_t$ and $\mathbf{a} = \mathbf{b} = k(\mathbf{x}, \mathbf{x})^{1/2}\mathbf{1}_t$, from (D.7) we have

$$(k(\mathbf{x}, \mathbf{x})\mathbf{1}_t\mathbf{1}_t^\top + \sigma^2\mathbf{I}_t)^{-1} = \sigma^{-2}\mathbf{I}_t - \frac{\sigma^{-4}k(\mathbf{x}, \mathbf{x})\mathbf{1}_t\mathbf{1}_t^\top}{1 + t\sigma^{-2}k(\mathbf{x}, \mathbf{x})}.$$

Therefore, we get

$$\begin{aligned} & (k(\mathbf{x}, \mathbf{x})\mathbf{1}_t)^\top (k(\mathbf{x}, \mathbf{x})\mathbf{1}_t\mathbf{1}_t^\top + \sigma^2\mathbf{I}_t)^{-1} (k(\mathbf{x}, \mathbf{x})\mathbf{1}_t) \\ &= \sigma^{-2}tk(\mathbf{x}, \mathbf{x})^2 - \frac{\sigma^{-4}t^2k(\mathbf{x}, \mathbf{x})^3}{1 + t\sigma^{-2}k(\mathbf{x}, \mathbf{x})} \\ &= \frac{\sigma^{-2}tk(\mathbf{x}, \mathbf{x})^2 + \sigma^{-4}t^2k(\mathbf{x}, \mathbf{x})^3}{1 + t\sigma^{-2}k(\mathbf{x}, \mathbf{x})} - \frac{\sigma^{-4}t^2k(\mathbf{x}, \mathbf{x})^3}{1 + t\sigma^{-2}k(\mathbf{x}, \mathbf{x})} \\ &= \frac{\sigma^{-2}tk(\mathbf{x}, \mathbf{x})^2}{1 + t\sigma^{-2}k(\mathbf{x}, \mathbf{x})}. \end{aligned} \quad (\text{D.8})$$

Hence, by substituting (D.8) into (D.1), we obtain

$$\begin{aligned} \zeta_t^2(\mathbf{x}) &= k(\mathbf{x}, \mathbf{x}) - (k(\mathbf{x}, \mathbf{x})\mathbf{1}_t)^\top (k(\mathbf{x}, \mathbf{x})\mathbf{1}_t\mathbf{1}_t^\top + \sigma^2\mathbf{I}_t)^{-1} (k(\mathbf{x}, \mathbf{x})\mathbf{1}_t) \\ &= k(\mathbf{x}, \mathbf{x}) - \frac{\sigma^{-2}tk(\mathbf{x}, \mathbf{x})^2}{1 + t\sigma^{-2}k(\mathbf{x}, \mathbf{x})} \\ &= \frac{k(\mathbf{x}, \mathbf{x}) + \sigma^{-2}tk(\mathbf{x}, \mathbf{x})^2}{1 + t\sigma^{-2}k(\mathbf{x}, \mathbf{x})} - \frac{\sigma^{-2}tk(\mathbf{x}, \mathbf{x})^2}{1 + t\sigma^{-2}k(\mathbf{x}, \mathbf{x})} \\ &= \frac{k(\mathbf{x}, \mathbf{x})}{1 + t\sigma^{-2}k(\mathbf{x}, \mathbf{x})}. \end{aligned}$$

Thus, for any $\mathbf{x} \in \Omega$, it holds that $\lim_{t \rightarrow \infty} \zeta_t^2(\mathbf{x}) = 0$. □

Next, we prove (Fact2).

Proof. From the definition of convergence in probability, it is sufficient to show that

$$\begin{aligned} & \forall \mathbf{x} \in \Omega, \forall a > 0, \forall \varepsilon \in (0, 1), \exists N(\mathbf{x}) \in \mathbb{N} \text{ s.t.} \\ & \forall n \geq N(\mathbf{x}), \text{P}(|\hat{\sigma}_n^2(\mathbf{x})| < a) > 1 - \varepsilon. \end{aligned} \quad (\text{D.9})$$

Let \mathbf{x} be an element of Ω , and let a be a positive number. In addition, let ε be a positive number with $\varepsilon \in (0, 1)$. Then, from (D.6), there exists a natural number $N_0(\mathbf{x}) \in \mathbb{N}$ such that the following inequality holds for any $N \geq N_0(\mathbf{x})$:

$$\zeta_N^2(\mathbf{x}) < a/2. \quad (\text{D.10})$$

Next, for a natural number K with $K \geq N_0(\mathbf{x})$, we evaluate $\hat{\sigma}_K^2(\mathbf{x})$. For a set of random variables $\mathcal{B} = \{\mathbf{B}_1, \dots, \mathbf{B}_l\}$, let

$$\hat{\sigma}_{\mathcal{B}}^2(\mathbf{x}) = k(\mathbf{x}, \mathbf{x}) - \hat{\mathbf{k}}_{\mathcal{B}}(\mathbf{x})^\top (\hat{\mathbf{K}}_{\mathcal{B}} + \sigma^2 \mathbf{I}_{|\mathcal{B}|})^{-1} \hat{\mathbf{k}}_{\mathcal{B}}(\mathbf{x}). \quad (\text{D.11})$$

Here, the j th element of $\hat{\mathbf{k}}_{\mathcal{B}}(\mathbf{x})$ is $k(\mathbf{B}_j, \mathbf{x})$, and the (u, v) th element is $k(\mathbf{B}_u, \mathbf{B}_v)$. Moreover, let $\mathcal{A} = \{\mathbf{A}_1, \dots, \mathbf{A}_K\}$. Then, we make a random variable $\tilde{\sigma}_K^2(\mathbf{x})$ to bound $\hat{\sigma}_K^2(\mathbf{x})$ as follows: If $|\hat{\sigma}_{\mathcal{A}'}^2(\mathbf{x}) - \zeta_{N_0(\mathbf{x})}^2(\mathbf{x})| \geq a/2$ for any $\mathcal{A}' \subset \mathcal{A}$ with $|\mathcal{A}'| = N_0(\mathbf{x})$, then we define $\tilde{\sigma}_K^2(\mathbf{x}) = k(\mathbf{x}, \mathbf{x})$. On the other hand, if $|\hat{\sigma}_{\mathcal{A}'}^2(\mathbf{x}) - \zeta_{N_0(\mathbf{x})}^2(\mathbf{x})| < a/2$ for some $\mathcal{A}' \subset \mathcal{A}$ with $|\mathcal{A}'| = N_0(\mathbf{x})$, then we define $\tilde{\sigma}_K^2(\mathbf{x}) = \hat{\sigma}_{\mathcal{A}'}^2(\mathbf{x})$. Therefore, from the definition of $\tilde{\sigma}_K^2(\mathbf{x})$, noting that the posterior variance in GP is monotonically non-increasing, we have

$$|\hat{\sigma}_K^2(\mathbf{x})| \leq |\tilde{\sigma}_K^2(\mathbf{x})|. \quad (\text{D.12})$$

Next, we prove that the following inequality holds for some large K :

$$\text{P}(|\zeta_{N_0(\mathbf{x})}^2(\mathbf{x}) - \tilde{\sigma}_K^2(\mathbf{x})| < a/2) > 1 - \varepsilon.$$

Let $\mathbf{A}_{j_1}, \dots, \mathbf{A}_{j_{N_0(\mathbf{x})}}$ be a sub-sequence of $\{\mathbf{A}_j\}_{j=1}^\infty$, and let $\mathcal{A}' \equiv \{\mathbf{A}_{j_1}, \dots, \mathbf{A}_{j_{N_0(\mathbf{x})}}\}$. Then, from (A3), there exists a positive number η such that $|\zeta_{N_0(\mathbf{x})}^2(\mathbf{x}) - \hat{\sigma}_{\mathcal{A}'}^2(\mathbf{x})| < a/2$ when $\mathbf{A}'_j (\in \mathcal{A}')$ satisfies $\mathbf{A}'_j \in \mathcal{N}(\mathbf{x}; \eta)$. In order to construct \mathcal{A}' , we consider a probability that at least one \mathbf{A}_j from \mathbf{A}_1 to \mathbf{A}_{K_1} satisfies $\mathbf{A}_j \in \mathcal{N}(\mathbf{x}; \eta)$. This probability is given by

$$1 - \text{P}(\mathbf{A}_1 \notin \mathcal{N}(\mathbf{x}; \eta) \wedge \dots \wedge \mathbf{A}_{K_1} \notin \mathcal{N}(\mathbf{x}; \eta)). \quad (\text{D.13})$$

Furthermore, $\text{P}(\mathbf{A}_2 \notin \mathcal{N}(\mathbf{x}; \eta) \wedge \dots \wedge \mathbf{A}_{K_1} \notin \mathcal{N}(\mathbf{x}; \eta))$ can be expressed as

$$\begin{aligned} & \text{P}(\mathbf{A}_2 \notin \mathcal{N}(\mathbf{x}; \eta) \wedge \dots \wedge \mathbf{A}_{K_1} \notin \mathcal{N}(\mathbf{x}; \eta)) \\ &= \text{P}(\mathbf{A}_2 \notin \mathcal{N}(\mathbf{x}; \eta)) \times \text{P}(\mathbf{A}_3 \notin \mathcal{N}(\mathbf{x}; \eta) | \mathbf{A}_2 \notin \mathcal{N}(\mathbf{x}; \eta)) \\ & \quad \times \\ & \quad \vdots \\ & \quad \times \\ & \text{P}(\mathbf{A}_{K_1} \notin \mathcal{N}(\mathbf{x}; \eta) | \mathbf{A}_l \notin \mathcal{N}(\mathbf{x}; \eta), l \in \{2, \dots, K_1 - 1\}). \end{aligned} \quad (\text{D.14})$$

Moreover, $\text{P}(\mathbf{A}_j \notin \mathcal{N}(\mathbf{x}; \eta) | \mathbf{A}_2 \notin \mathcal{N}(\mathbf{x}; \eta) \wedge \dots \wedge \mathbf{A}_{j-1} \notin \mathcal{N}(\mathbf{x}; \eta))$ can be written as follows:

$$\begin{aligned} & \text{P}(\mathbf{A}_j \notin \mathcal{N}(\mathbf{x}; \eta) | \mathbf{A}_2 \notin \mathcal{N}(\mathbf{x}; \eta) \wedge \dots \wedge \mathbf{A}_{j-1} \notin \mathcal{N}(\mathbf{x}; \eta)) \\ &= 1 - \text{P}(\mathbf{A}_j \in \mathcal{N}(\mathbf{x}; \eta) | \mathbf{A}_l \notin \mathcal{N}(\mathbf{x}; \eta), l \in \{2, \dots, j-1\}). \end{aligned} \quad (\text{D.15})$$

In addition, from (A2), there exists $\mathbf{x}^* \in \Omega$ and c_i such that $\text{P}(\mathbf{S}(\mathbf{x}^*, c_i) \in \mathcal{N}(\mathbf{x}; \eta)) \equiv q > 0$. Hence, by noting that Line 11–12 in Algorithm 1, we have

$$\begin{aligned} & \text{P}(\mathbf{A}_j \in \mathcal{N}(\mathbf{x}; \eta) | \mathbf{A}_2 \notin \mathcal{N}(\mathbf{x}; \eta) \wedge \dots \wedge \mathbf{A}_{j-1} \notin \mathcal{N}(\mathbf{x}; \eta)) \\ & \geq \text{P}(r_j = 1 \wedge C_j = (\mathbf{x}^*, c_i) \wedge \mathbf{S}(\mathbf{x}^*, c_i) \in \mathcal{N}(\mathbf{x}; \eta) | \mathbf{A}_2 \notin \mathcal{N}(\mathbf{x}; \eta) \wedge \dots \wedge \mathbf{A}_{j-1} \notin \mathcal{N}(\mathbf{x}; \eta)) \\ & = \text{P}(r_j = 1) \text{P}(\mathbf{S}(\mathbf{x}^*, c_i) \in \mathcal{N}(\mathbf{x}; \eta)) \text{P}(C_j = (\mathbf{x}^*, c_i)) \\ & \geq p_j q \kappa_{min}, \end{aligned} \quad (\text{D.16})$$

where $\kappa_{min} = \min\{\kappa_1, \dots, \kappa_k\} > 0$. Therefore, from (D.14), (D.15) and (D.16), we get

$$\text{P}(\mathbf{A}_2 \notin \mathcal{N}(\mathbf{x}; \eta) \wedge \dots \wedge \mathbf{A}_{K_1} \notin \mathcal{N}(\mathbf{x}; \eta)) \leq \prod_{j=2}^{K_1} (1 - p_j q \kappa_{min}). \quad (\text{D.17})$$

Moreover, by noting that e^x can be expanded as $e^x = 1 + x + x^2 e^{x^*} / 2$, we obtain the following inequality:

$$e^{-p_j q \kappa_{\min}} = 1 - p_j q \kappa_{\min} + c_{>0} \geq 1 - p_j q \kappa_{\min},$$

where $c_{>0}$ is a positive constant. Thus, by substituting this inequality to (D.17), we have

$$\mathbb{P}(\mathbf{A}_2 \notin \mathcal{N}(\mathbf{x}; \eta) \wedge \cdots \wedge \mathbf{A}_{K_1} \notin \mathcal{N}(\mathbf{x}; \eta)) \leq \prod_{j=2}^{K_1} e^{-p_j q \kappa_{\min}} = e^{-q \kappa_{\min} \sum_{j=2}^{K_1} p_j}. \quad (\text{D.18})$$

Hence, by combining (D.13) and (D.18), the following holds:

$$\begin{aligned} & 1 - \mathbb{P}(\mathbf{A}_1 \notin \mathcal{N}(\mathbf{x}; \eta) \wedge \cdots \wedge \mathbf{A}_{K_1} \notin \mathcal{N}(\mathbf{x}; \eta)) \\ & \geq 1 - \mathbb{P}(\mathbf{A}_2 \notin \mathcal{N}(\mathbf{x}; \eta) \wedge \cdots \wedge \mathbf{A}_{K_1} \notin \mathcal{N}(\mathbf{x}; \eta)) \\ & \geq 1 - e^{-q \kappa_{\min} \sum_{j=2}^{K_1} p_j}. \end{aligned}$$

Thus, from (A1), there exists a natural number K_1 such that $e^{-q \kappa_{\min} \sum_{j=2}^{K_1} p_j} < \varepsilon / N_0(\mathbf{x})$. This implies that the probability which at least one \mathbf{A}_j from \mathbf{A}_1 to \mathbf{A}_{K_1} satisfies $\mathbf{A}_j \in \mathcal{N}(\mathbf{x}; \eta)$ is greater than $1 - \varepsilon / N_0(\mathbf{x})$. Similarly, there exists a natural number K_2 such that the probability which at least one $\mathbf{A}_{j'}$ from \mathbf{A}_{K_1+1} to \mathbf{A}_{K_2} satisfies $\mathbf{A}_{j'} \in \mathcal{N}(\mathbf{x}; \eta)$ is greater than $1 - \varepsilon / N_0(\mathbf{x})$. By repeating the same argument, we have $K_1, K_2, K_3, \dots, K_{N_0(\mathbf{x})}$. Let $K = K_{N_0(\mathbf{x})}$, and let $\mathcal{A}_1 = \{\mathbf{A}_1, \dots, \mathbf{A}_{K_1}\}, \mathcal{A}_2 = \{\mathbf{A}_{K_1+1}, \dots, \mathbf{A}_{K_2}\}, \dots, \mathcal{A}_{N_0(\mathbf{x})} = \{\mathbf{A}_{K_{N_0(\mathbf{x})-1}+1}, \dots, \mathbf{A}_K\}$. Then, it holds that

$$\begin{aligned} & \{\exists \mathbf{A}_{j_1} \in \mathcal{A}_1, \mathbf{A}_{j_1} \in \mathcal{N}(\mathbf{x}; \eta)\} \cap \{\exists \mathbf{A}_{j_2} \in \mathcal{A}_2, \mathbf{A}_{j_2} \in \mathcal{N}(\mathbf{x}; \eta)\} \cap \cdots \cap \{\exists \mathbf{A}_{j_{N_0(\mathbf{x})}} \in \mathcal{A}_{N_0(\mathbf{x})}, \mathbf{A}_{j_{N_0(\mathbf{x})}} \in \mathcal{N}(\mathbf{x}; \eta)\} \\ & \Rightarrow |\varsigma_{N_0(\mathbf{x})}^2(\mathbf{x}) - \hat{\sigma}_{\{\mathbf{A}_{j_1}, \mathbf{A}_{j_2}, \dots, \mathbf{A}_{j_{N_0(\mathbf{x})}}\}}^2(\mathbf{x})| < a/2 \\ & \Rightarrow |\varsigma_{N_0(\mathbf{x})}^2(\mathbf{x}) - \tilde{\sigma}_K^2(\mathbf{x})| < a/2. \end{aligned}$$

Thus, $\mathbb{P}(|\varsigma_{N_0(\mathbf{x})}^2(\mathbf{x}) - \tilde{\sigma}_K^2(\mathbf{x})| < a/2)$ can be bounded as

$$\begin{aligned} & \mathbb{P}(|\varsigma_{N_0(\mathbf{x})}^2(\mathbf{x}) - \tilde{\sigma}_K^2(\mathbf{x})| < a/2) \\ & \geq \mathbb{P}(\{\exists \mathbf{A}_{j_1} \in \mathcal{A}_1, \mathbf{A}_{j_1} \in \mathcal{N}(\mathbf{x}; \eta)\} \cap \{\exists \mathbf{A}_{j_2} \in \mathcal{A}_2, \mathbf{A}_{j_2} \in \mathcal{N}(\mathbf{x}; \eta)\} \cap \cdots \\ & \quad \cap \{\exists \mathbf{A}_{j_{N_0(\mathbf{x})}} \in \mathcal{A}_{N_0(\mathbf{x})}, \mathbf{A}_{j_{N_0(\mathbf{x})}} \in \mathcal{N}(\mathbf{x}; \eta)\}) \\ & \geq \left\{ \sum_{v=1}^{N_0(\mathbf{x})} \mathbb{P}(\exists \mathbf{A}_{j_v} \in \mathcal{A}_v, \mathbf{A}_{j_v} \in \mathcal{N}(\mathbf{x}; \eta)) \right\} - (N_0(\mathbf{x}) - 1) \\ & > \left\{ \sum_{v=1}^{N_0(\mathbf{x})} (1 - \varepsilon / N_0(\mathbf{x})) \right\} - (N_0(\mathbf{x}) - 1) = 1 - \varepsilon. \end{aligned} \quad (\text{D.19})$$

Finally, we consider (D.12). From the triangle inequality, we have

$$|\hat{\sigma}_K^2(\mathbf{x})| \leq |\tilde{\sigma}_K^2(\mathbf{x})| = |\tilde{\sigma}_K^2(\mathbf{x}) - \varsigma_{N_0(\mathbf{x})}^2(\mathbf{x}) + \varsigma_{N_0(\mathbf{x})}^2(\mathbf{x})| \leq |\tilde{\sigma}_K^2(\mathbf{x}) - \varsigma_{N_0(\mathbf{x})}^2(\mathbf{x})| + |\varsigma_{N_0(\mathbf{x})}^2(\mathbf{x})|.$$

This implies that

$$\{|\tilde{\sigma}_K^2(\mathbf{x}) - \varsigma_{N_0(\mathbf{x})}^2(\mathbf{x})| < a/2\} \cap \{|\varsigma_{N_0(\mathbf{x})}^2(\mathbf{x})| < a/2\} \Rightarrow \{|\hat{\sigma}_K^2(\mathbf{x})| < a\}.$$

Therefore, by using (D.10) and (D.19), it holds that

$$\begin{aligned} \mathbb{P}(|\hat{\sigma}_K^2(\mathbf{x})| < a) & \geq \mathbb{P}(\{|\tilde{\sigma}_K^2(\mathbf{x}) - \varsigma_{N_0(\mathbf{x})}^2(\mathbf{x})| < a/2\} \cap \{|\varsigma_{N_0(\mathbf{x})}^2(\mathbf{x})| < a/2\}) \\ & \geq \mathbb{P}(|\tilde{\sigma}_K^2(\mathbf{x}) - \varsigma_{N_0(\mathbf{x})}^2(\mathbf{x})| < a/2) + \mathbb{P}(|\varsigma_{N_0(\mathbf{x})}^2(\mathbf{x})| < a/2) - 1 \\ & > 1 - \varepsilon + 1 - 1 = 1 - \varepsilon. \end{aligned}$$

Furthermore, for any K' with $K' \geq K$, it holds that $|\hat{\sigma}_{K'}^2(\mathbf{x})| \geq |\hat{\sigma}_K^2(\mathbf{x})|$ because posterior variances of GP are non-increasing. Hence, noting that

$$|\hat{\sigma}_K^2(\mathbf{x})| < a \Rightarrow |\hat{\sigma}_{K'}^2(\mathbf{x})| < a,$$

we have

$$\mathbb{P}(|\hat{\sigma}_{K'}^2(\mathbf{x})| < a) \geq \mathbb{P}(|\hat{\sigma}_K^2(\mathbf{x})| < a) > 1 - \varepsilon.$$

Consequently, $\hat{\sigma}_t^2(\mathbf{x})$ converges in probability to zero. \square

Next, we prove (Fact3).

Proof. From (Fact2), $\hat{\sigma}_t^2(\mathbf{x})$ converges in probability to zero. Furthermore, it is known that if a random variable sequence F_1, F_2, \dots converges in probability to α , then there exists a sub-sequence F_{n_1}, F_{n_2}, \dots such that F_{n_1}, F_{n_2}, \dots converges to α almost surely (see, e.g., [18]). Hence, there exists a sub-sequence $\hat{\sigma}_{n_1}^2(\mathbf{x}), \hat{\sigma}_{n_2}^2(\mathbf{x}), \dots$ such that

$$\hat{\sigma}_{n_t}^2(\mathbf{x}) \xrightarrow{\text{a.s.}} 0, \quad (\text{as } t \rightarrow \infty). \quad (\text{D.20})$$

In addition, noting that posterior variances of GP are non-increasing, $\hat{\sigma}_t^2(\mathbf{x})$ satisfies that $\hat{\sigma}_1^2(\mathbf{x}) \geq \hat{\sigma}_2^2(\mathbf{x}) \geq \dots \geq 0$. Thus, by using this inequality and (D.20), we have

$$\hat{\sigma}_t^2(\mathbf{x}) \xrightarrow{\text{a.s.}} 0, \quad (\text{as } t \rightarrow \infty). \quad (\text{D.21})$$

□

Finally, we prove the second half of Theorem 5.2.

Proof. For any $\mathbf{x} \in \Omega$, (D.21) can be expressed as follows:

$$\begin{aligned} & \hat{\sigma}_t^2(\mathbf{x}) \xrightarrow{\text{a.s.}} 0, \quad (\text{as } t \rightarrow \infty) \\ & \Leftrightarrow \exists \text{ event } E_{\mathbf{x}} \in \mathcal{B} \text{ s.t. } \mathbb{P}(E_{\mathbf{x}}) = 1, \quad \forall \omega \in E_{\mathbf{x}}, \quad \lim_{t \rightarrow \infty} (\hat{\sigma}_t^2(\mathbf{x}))(\omega) = 0, \end{aligned}$$

where \mathcal{B} is a σ -field of a probability space $(\mathcal{S}, \mathcal{B}, \mathbb{P})$, and $(\hat{\sigma}_t^2(\mathbf{x}))(\omega)$ is the observed value of the random variable $\hat{\sigma}_t^2(\mathbf{x})$ at the point $\omega \in \mathcal{S}$. By using $E_{\mathbf{x}}$, we define an event E as

$$E \equiv \bigcap_{\mathbf{x} \in \Omega} E_{\mathbf{x}}.$$

From the definition of E , the following holds:

$$E \in \mathcal{B}, \quad \mathbb{P}(E) = 1, \quad \forall \omega \in E, \quad \forall \mathbf{x} \in \Omega, \quad \lim_{t \rightarrow \infty} (\hat{\sigma}_t^2(\mathbf{x}))(\omega) = 0. \quad (\text{D.22})$$

Hence, from the classification rule (3.1), if $\beta^{1/2}\sigma_t(\mathbf{x}) < \epsilon$ for any $\mathbf{x} \in \Omega$, then all the points are classified. Thus, noting that β is positive, it is sufficient to show that $\sigma_t^2(\mathbf{x}) < \epsilon^2\beta^{-1}$. Since $\sigma_t^2(\mathbf{x})$ is the observed value of $\hat{\sigma}_t^2(\mathbf{x})$, from (D.22), there exists a natural number $N_{\omega, \mathbf{x}} \in \mathbb{N}$ such that $(\hat{\sigma}_{N_{\omega, \mathbf{x}}}^2(\mathbf{x}))(\omega) < \epsilon^2\beta^{-1}$ for any $\omega \in E$ and $\mathbf{x} \in \Omega$. Therefore, by letting $N_{\omega} = \max_{\mathbf{x} \in \Omega} N_{\omega, \mathbf{x}}$, it holds that $(\hat{\sigma}_{N_{\omega}}^2(\mathbf{x}))(\omega) < \epsilon^2\beta^{-1}$ for any $\mathbf{x} \in \Omega$. This implies that

$$\exists \text{ event } E \in \mathcal{B}, \quad \mathbb{P}(E) = 1$$

and

$$\forall \omega \in E, \quad \exists N_{\omega} \in \mathbb{N} \text{ s.t. } \forall \mathbf{x} \in \Omega, \quad (\hat{\sigma}_{N_{\omega}}^2(\mathbf{x}))(\omega) \equiv \sigma_{N_{\omega}}^2(\mathbf{x}) < \epsilon^2\beta^{-1}.$$

Consequently, we have the second half of Theorem 5.2. □

E. Additional numerical experiments

E.1. Effect of probability p_t

In this subsection, we confirm the difference in behavior due to the difference in probability p_t through a two-dimensional synthetic function. We first set Ω as a grid point that is obtained by uniformly cutting the region $[-5, 5] \times [-5, 5]$ into 30×30 . As the kernel function, we used Gaussian kernel $k(\mathbf{x}, \mathbf{x}') = \sigma_f^2 \exp(-\|\mathbf{x} - \mathbf{x}'\|_2^2/L)$. Furthermore, we used the error variance $\sigma^2 = 10^{-4}$, the accuracy parameter $\epsilon = 10^{-12}$ and $\beta^{1/2} = 1.96$. In this experiment, we considered two costs $c_1 = 1$ and $c_2 = 2$. For each c_i and $\mathbf{x} = (x_1, x_2)^\top \in \Omega$, the following was used as $\mathbf{S}(\mathbf{x}, c_i)$:

$$\mathbf{S}(\mathbf{x}, c_i) = (\mathcal{U}_{[L_1(\mathbf{x}, c_i), U_1(\mathbf{x}, c_i)]}, \mathcal{U}_{[L_2(\mathbf{x}, c_i), U_2(\mathbf{x}, c_i)]})^\top,$$

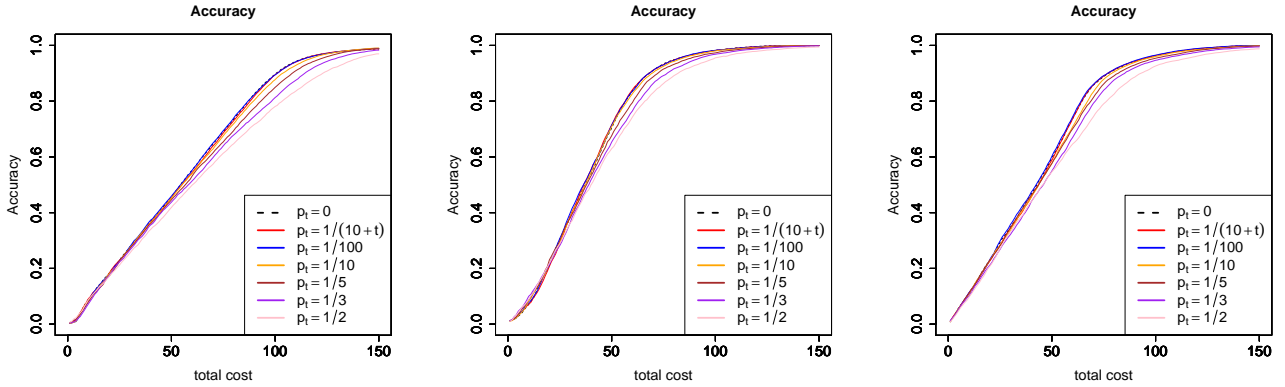


Figure 4: Average accuracy based on 20 Monte Carlo simulations in cases 1 to 3. The left, center and right figure show the Case1, Case2 and Case3, respectively.

where $\mathcal{U}_{[a,b]}$ is a uniform distribution on $[a, b]$, and

$$\begin{aligned} L_1(\mathbf{x}, c_i) &= \max\{(x_1 - \zeta^{(i)}), -5\}, \\ U_1(\mathbf{x}, c_i) &= \min\{(x_1 + \zeta^{(i)}), 5\}, \\ L_2(\mathbf{x}, c_i) &= \max\{(x_2 - \zeta^{(i)}), -5\}, \\ U_2(\mathbf{x}, c_i) &= \min\{(x_2 + \zeta^{(i)}), 5\}. \end{aligned}$$

Here, we set $\zeta^{(1)} = 1/2.9$ and $\zeta^{(2)} = 0.05$. Moreover, we assumed that $\mathcal{U}_{[L_1(\mathbf{x}, c_i), U_1(\mathbf{x}, c_i)]}$ and $\mathcal{U}_{[L_2(\mathbf{x}, c_i), U_2(\mathbf{x}, c_i)]}$ are mutually independent. Then, by letting $p_t = 0$, $p_t = 1/(10+t)$ and $p_t = 1/a$, $a \in \{2, 3, 5, 10, 100\}$, we confirmed the behavior when each probability was used. In addition, we also set $\kappa_1 = (1 - |\Omega|10^{-8})/|\Omega|$ and $\kappa_2 = 10^{-8}$. For true functions, kernel parameters and thresholds, we considered the following three cases:

(Case1) True function: $f(x_1, x_2) = x_1^2 + x_2^2$, kernel parameters: $\sigma_f^2 = 225$, $L = 2$, threshold: $h = 20$.

(Case2) True function: $f(x_1, x_2) = -(x_1^2 + x_2 - 11)^2 - (x_1 + x_2^2 - 7)^2$, kernel parameters: $\sigma_f^2 = 3000$, $L = 2$, threshold: $h = -50$.

(Case3) True function: $f(x_1, x_2) = \sum_{j=1}^2 (x_j^4 - 16x_j^2 + 5x_j)/2$, kernel parameters: $\sigma_f^2 = 900$, $L = 2$, threshold: $h = -10$.

In order to compute integrals, we used the approximation method based on (B.2). Note that the discrete distribution $\hat{\mathbf{S}}(\mathbf{x}, c_i)$ can be derived analytically in the settings of this subsection. Under this setting, one initial point was taken at random, and points were acquired until the total cost reached 150. The average obtained by 20 Monte Carlo simulations is given in Figure 4. From Figure 4, we can confirm that p_t for establishing the theoretical guarantee does not have a dramatic effect on the result if a sufficiently small value is set. Moreover, we can also confirm that the proposed method can achieve high accuracy at low cost.

E.2. Synthetic experiments

In this subsection, we compare the proposed method with some existing methods using synthetic functions. Hereafter, for simplicity, we used $p_t = 0$.

E.2.1. Two-dimensional Rosenbrock function

We also considered the 2-dimensional Rosenbrock function (reduced to 1/100 and moved)

$$f(x_1, x_2) = (x_2 - x_1^2)^2 + (1 - x_1)^2/100 - 5$$

as the true function, and defined the grid point obtained by uniformly cutting the region $[-2, 2] \times [-1, 3]$ into 40×40 as Ω . Furthermore, we used the Gaussian kernel with $\sigma_f^2 = 64$ and $L = 0.5$. In addition, we set

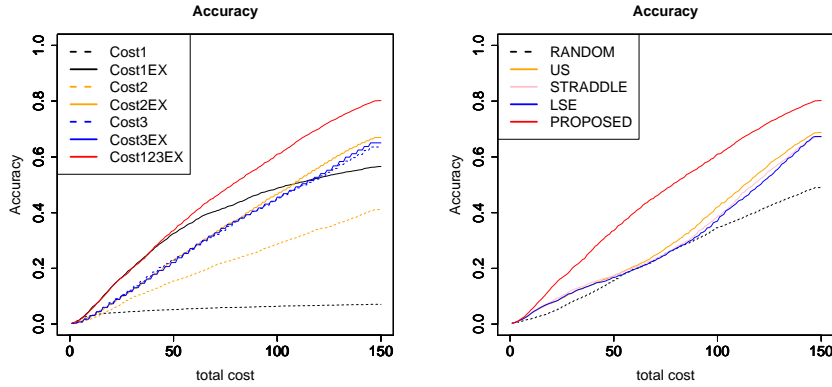


Figure 5: Average accuracy based on 20 Monte Carlo simulations in the Rosenbrock function. The left figure shows the influence of integration against the input distribution and that of cost in evaluating the input point. The right figure shows the result of comparison with existing methods.

$\sigma^2 = 0.25$, $h = 0$, $\epsilon = 10^{-12}$ and $\beta^{1/2} = 1.96$. Similarly in this experiment, we considered three costs $c_1 = 1$, $c_2 = 2$ and $c_3 = 3$. Moreover, for each c_i and $\mathbf{x} = (x_1, x_2)^\top \in \Omega$, we assumed that

$$\mathbf{S}(\mathbf{x}, c_i) = \mathbf{x} + (G_{[0,2-x_1]}(\zeta^{(i)}, 1), G_{[0,3-x_2]}(\zeta^{(i)}, 1))^\top,$$

where $G_{[0,2-x_1]}(\zeta^{(i)}, 1)$ and $G_{[0,3-x_2]}(\zeta^{(i)}, 1)$ are independent. Furthermore, we used $\zeta^{(1)} = 4$, $\zeta^{(2)} = 1$, $\zeta^{(3)} = 0.01$. Under this setting, we performed similar experiments to Subsubsection 6.1.1. From Figure 5, even in the case of the Rosenbrock function, we can see that the proposed method has higher accuracy than the other methods.

E.2.2. One-dimensional function and unknown input distributions

Here, we considered the one dimensional function

$$f(x) = \cos(10x) + \sin(12x) + x^2/10$$

as the true function, and defined the grid point observed by uniformly cutting the interval $[0, 5]$ into 100 as Ω . In addition, we used the Gaussian kernel with $\sigma_f^2 = 2$ and $L = 0.1$. Furthermore, we set $\sigma^2 = 10^{-4}$, $h = 0.4$, $\epsilon = 10^{-12}$ and $\beta^{1/2} = 3$. In this experiment, we considered two costs $c_1 = 1$ and $c_2 = 2$. Moreover, for each c_i and $x \in \Omega$, we defined that

$$S(x, c_i) = x + \mathcal{N}(\mu_{c_i}, \sigma_{c_i}^2),$$

where $(\mu_{c_1}, \sigma_{c_1}^2)^\top = (2, 0.16)^\top$ and $(\mu_{c_2}, \sigma_{c_2}^2)^\top = (0, 10^{-4})^\top$. Then, we considered the following three cases:

Case1 Assume that μ_{c_i} and $\sigma_{c_i}^2$ are unknown and known, respectively. Moreover, we used $\mu_{c_i} \sim \mathcal{N}(\mu_{c_i,0}, \sigma_{c_i,0}^2)$ as a prior distribution of μ_{c_i} , where $(\mu_{c_1,0}, \sigma_{c_1,0}^2)^\top = (0.5, 0.1)^\top$ and $(\mu_{c_2,0}, \sigma_{c_2,0}^2)^\top = (0.15, 0.03)^\top$.

Case2 Assume that μ_{c_i} and $\sigma_{c_i}^2$ are known and unknown, respectively. In addition, we used $\sigma_{c_i}^{-2} \sim \mathcal{G}(\alpha_{c_i,0}, \beta_{c_i,0})$ as a prior of $\sigma_{c_i}^{-2}$, where $(\alpha_{c_1,0}, \beta_{c_1,0})^\top = (2, 2)^\top$ and $(\alpha_{c_2,0}, \beta_{c_2,0})^\top = (5, 1)^\top$.

Case3 Assume that both μ_{c_i} and $\sigma_{c_i}^2$ are unknown. Moreover, we used $\mu_{c_i} \sim \mathcal{N}(\mu_{c_i,0}, \sigma_{c_i,0}^2/\kappa_{c_i,0})$ and $\sigma_{c_i}^{-2} \sim \mathcal{G}(\alpha_{c_i,0}, \beta_{c_i,0})$ respectively as priors of μ_{c_i} and $\sigma_{c_i}^{-2}$, where $(\mu_{c_1,0}, \kappa_{c_1,0}, \alpha_{c_1,0}, \beta_{c_1,0})^\top = (0.5, 1, 2, 2)^\top$ and $(\mu_{c_2,0}, \kappa_{c_2,0}, \alpha_{c_2,0}, \beta_{c_2,0})^\top = (0.15, 1, 5, 1)^\top$.

Note that in Case1, $g_t(x|\boldsymbol{\theta}_x^{(c_i)})$ is a density function with normal distribution, and also note that in Case2-3, $g_t(x|\boldsymbol{\theta}_x^{(c_i)})$ is a density function with t -distribution (see, e.g., [2]). Under this setting, we performed similar experiments until the total cost reached 100, where we used the approximation (B.1) with $M = 1000$. The average obtained by 50 Monte Carlo simulations is given in Figure 6. From Figure 6, we can confirm that the proposed method has higher accuracy than other existing methods. Similarly, Figure 7 shows the accuracy when the true density function, estimated function $g_t(x|\boldsymbol{\theta}_x^{(c_i)})$ and not-estimated function (i.e., $g_0(x|\boldsymbol{\theta}_x^{(c_i)})$)

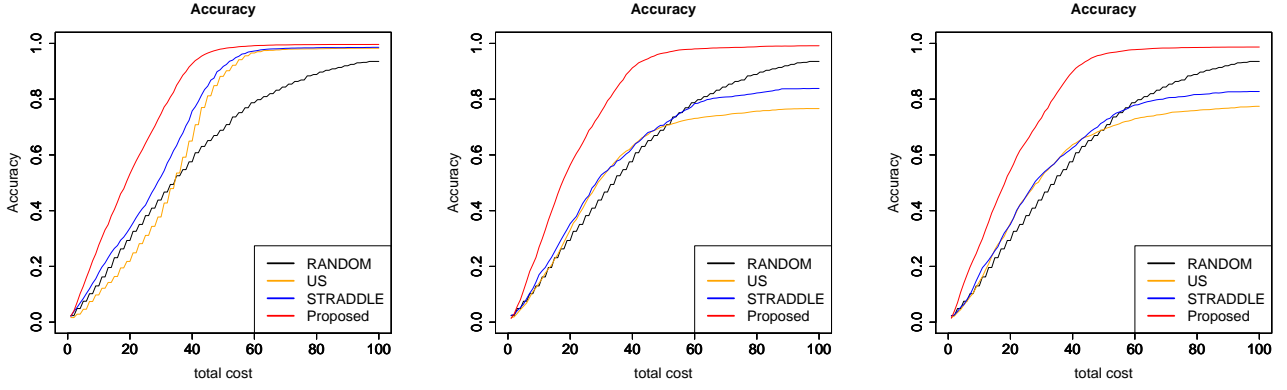


Figure 6: Average accuracy based on 50 Monte Carlo simulations in case1-3. The left, center and right figure show the Case1, Case2 and Case3, respectively.

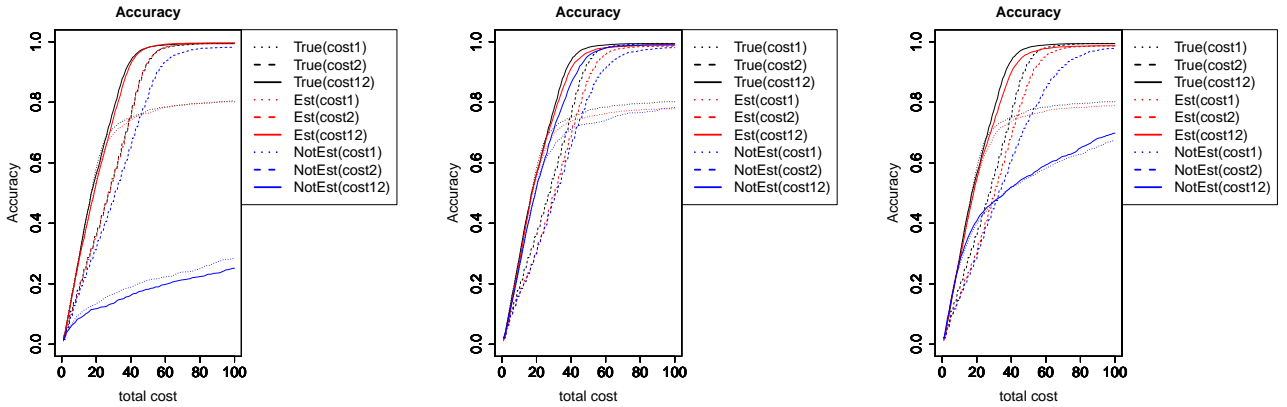


Figure 7: Average accuracy based on 50 Monte Carlo simulations in case1-3. The left, center and right figure show the Case1, Case2 and Case3, respectively. Moreover, True, Est, and NotEst indicate the results when the true density function is known, when parameter estimation is performed, and when parameter estimation is not performed.

are used as an approximation of $g(x|\theta_x^{(c_i)})$ in (B.1). From Figure 7, we can see that when parameter estimation is not performed, efficient classification can not be performed. On the other hand, it can be confirmed that accuracy improvement has been achieved by parameter estimation. In particular, in the case of this experimental, it can be confirmed that performance equivalent to that obtained when the true distribution was known was achieved by parameter estimation.